SUPPORTING INFORMATION

Vibrationally Hot and Cold Triplets. Sensitizer-Dependent Dynamics and Localized Vibrational Promotion of a Di-π-methane Rearrangement.

Kai-Yuan Kuan and Daniel A. Singleton*

Department of Chemistry, Texas A&M University, 3255 TAMU,
College Station, Texas 77843, United States
singleton@chem.tamu.edu

Experimental Procedures

General Methods.

Benzobarrelene (**1**) was prepared as described by Hales[1] and used in each case within one week of preparation. All other chemicals were used as commercially available. The photochemical reactions were conducted in a Rayonet Photochemical Reactor equipped with RPR-3000Å lamps. The internal temperature of reactions was monitored internally using a digital thermometer, and the temperatures reported reflect an approximate average temperature within ~± 5 degrees. The 300 K temperature was obtained using a fan to cool the Rayonet.

Di-π-methane Rearrangements of Benzobarrelene (1).

Acetophenone-Sensitized Reaction at 200 K

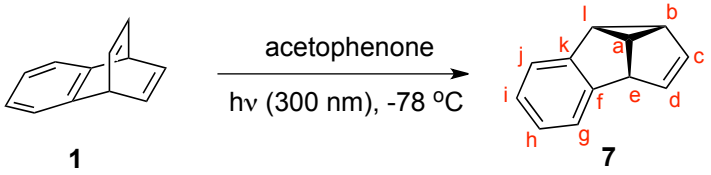

1 **7**

A mixture of 1.0 g (6.5 mmol) of freshly prepared **1** and 7.8 g (65 mmol) of acetophenone was prepared in 300 mL of anhydrous diethyl ether. The mixture was placed in a 500-mL Pyrex® bottle equipped with a cold finger (see Figure S1). The reaction mixture was added to the external container with dry ice /acetone filled in the inner container. The reaction was irradiated by 300 nm light while at -70 ºC until 75% conversion was reached based on ^{1}H NMR analysis of an aliquot. This required ~10-12 h. The reaction mixture was concentrated on a rotary evaporator, and most of the acetophenone was then removed by vacuum distillation (60 ºC, 1.3 Torr). The crude benzosemibullvalene product (**7**) was further purified on a 20 mm by 400 mm basic alumina column using petroleum ether as eluent to afford 312 mg (31%) of **7**. The ^{1}H and ^{13}C NMR spectra were in accord with previous report, and the important peak assignments were confirmed based on HSQC spectra.[2]

^{1}H NMR ($CDCl_3$, 500 MHz): 7.20-7.10 (m, 2H), 6.94-6.87 (m, 2H), 5.62 (ddd, J = 5.1, 2.2, 0.57 Hz, 1H), 5.23 (dd, J = 5.1, 2.5 Hz, 1H), 3.92 (dd, J = 6.3, 2.3 Hz, 1H), 3.3 (qd, J = 6.3,

0.57 Hz), 3.1 (t, J = 6.6 Hz, 1H), 2.7 (td, J = 6.6, 0.44 Hz, 1H)

^{13}C NMR ($CDCl_3$, 125 MHz): 150.1 (f / k), 137.1 (f / k), 135.5 (d), 126.0 (h / i), 125.2 (h / i), 125.1 (g), 121.0 (c), 120.8 (j), 53.8 (e), 47.7 (a), 39.6 (b), 37.4 (l).

Of note, the relative positions of carbons c and j change with solvent: ^{13}C NMR (acetone-D_6, 125 MHz): 150.4 (f / k), 137.5 (f / k), 135.7 (d), 126.0 (g / h / i), 125.3 (g / h / i), 125.2 (g / h / i), 121.1 (j), 120.9 (c), 53.9 (e), 47.9 (a), 39.7 (b), 37.5 (l).

Figure S1. Experimental set-up for low temperature photolyses.

Acetone-Sensitized Reaction at 200 K

A mixture of 1.0 g (6.5 mmol) of **1** in 20 mL of acetone was added to a 30-cm × 1-cm quartz tube. The reaction mixture was cooled in a dry ice / isopropanol bath in a 30-cm × 10-cm quartz tube (see Figure S2). The reaction was irradiated by 300 nm light while at -70 ºC until 75% conversion was reached based on ^{1}H NMR analysis of an aliquot. This required ~25-30 h. The reaction mixture was concentrated on a rotary evaporator. The residue was chromatographed on a 20 mm by 400 mm alumina column using petroleum ether as eluent to afford 478 mg (48%) of **7**.

Acetophenone-Sensitized Reaction at 300 K

A mixture of 1.0 g (6.5 mmol) of **1** and 7.8 g (65 mmol) of acetophenone in 20 mL of anhydrous diethyl ether was added to a 30-cm by 1-cm quartz tube. The reaction was irradiated by 300 nm light until 75% conversion was reached based on ^{1}H NMR analysis of an aliquot. This required 5 h. The reaction mixture was concentrated on a rotary evaporator and vacuum distilled to remove most of the acetophenone (60 ºC, 1.3 Torr). The residue was chromatographed on a 20 mm by 400 mm alumina column using petroleum ether as eluent to afford 291 mg (29%) of **7**.

Acetone-Sensitized Reaction at 300 K

A mixture of 1.0 g (6.5 mmol) of **1** in 20 mL of acetone was placed in a 30-cm by 1-cm quartz tube and was irradiated with 300 nm light until 75% conversion measured by ^{1}H NMR, which took 3 days. The reaction mixture was concentrated on a rotary evaporator to remove acetone. The residue was chromatographed on a 20 mm by 400 mm alumina column using petroleum ether to afford 267 mg (27%) of **7**.

Methyl-Benzoate Sensitized Reaction at 300 K

A 1.0 g (6.5 mmol) of **1** was dissolved in 20 mL of methyl benzoate in a 30-cm by 1-cm quartz tube. The reaction was irradiated by 300 nm light until 75% conversion was reached based on ^{1}H NMR analysis of an aliquot. Because of minimal absorption of the nominally 300 nm light, this required 21 days. Most of the methyl benzoate was then removed by vacuum distillation (80 ºC, 1.3 Torr), and the crude benzosemibullvalene product (**7**) was chromatographed through a 20 mm by 400 mm alumina column using petroleum ether as eluent to afford 353 mg (35%) of **7**.

KIE measurements

Peak Assignments

The key ^{13}C NMR signals for **7** were assigned as shown in Figure S2 based on ^{1}H and HSQC spectra. The numbers in Figure S2 refer to the order of the peaks from downfield to upfield in the spectra in each solvent. In $CDCl_3$, the peak of the ortho carbon away from the cyclopropane ring (g) is upfield from the alkene carbon closer to the ring (c). Due to the proximity of the two peaks in $CDCl_3$, most KIE measurements were based on samples in acetone-d_6 instead of $CDCl_3$.

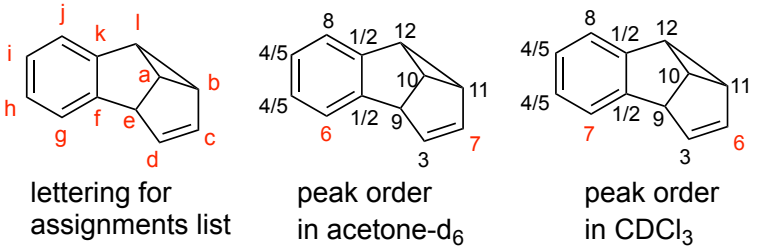

Figure S2. Lettering for assignments list and peak order in aceton-d_6 and $CDCl_3$.

NMR Details for KIE Measurements

The ^{13}C spectra were recorded at 125.7 MHz using inverse gated decoupling and calibrated $\pi/2$ pulses. The delay between pulses ranged from 36.5 to 41.5 s, and the number of points collected per FID ranged from 387,000 to 524,000. The FID acquisition times ranged from 6.5 to 8.4 s. The integrations were obtained numerically by a macro provided in a later section. A zero-order baseline correction was generally applied, but to avoid any qualitative manipulation no first-order or higher-order baseline correction was ever applied.

For each KIE measurement, the center of the spectrum was placed at the middle of the two peaks of interests, which were carbons 3 and 7 in most cases. The spectral widths were set to ensure that no peak of **7** was within 10% of the spectral edge. T_1 measurements were carried out on each sample, and the relaxation time between each pulse was set to be more than 7 times T_1.

The integration ranges for each peak of interest were chosen based on the T_1 measurements with the goal of including an equal percentage of each peak's integration, typically 99.7% for each. For calculating this percentage, it was assumed that each peak's shape was a combination of a Lorentzian, based on the T_1 with a width of $1/(\pi\ T_1)$, with narrower gaussian broadenings from imperfect shims.

For the integrations of the peaks for carbon 3 versus carbon 7 (see the assignments below) for **7**, the integration of carbon 7 was set to 1000 and the integration of carbon 3 was recorded. The raw results are at the top of Table S1. Because of the close proximity of carbons g and c, in some of the spectra the integration range of carbon c included a satellite peak from carbon g. For these spectra, the integrations were adjusted by an assumed natural abundance of

^{13}C of 1.07%. (Any reasonable choice makes no more than round-off changes in the KIEs.)

Table S1. Intramolecular KIE Results for **7** obtained from Di-π-methane rearrangement.

sensitizer	acetophenone	acetone	methyl benzoate	acetophenone	acetone
temperature	300 K	300 K	300 K	200 K	200 K
entry			Raw Integration Results		
1	1075.32	1017.48	1036.07	1142.03	1057.58
2	1073.66	1025.87	1049.39	1135.64	1049.77
3	1051.91	1017.36	1044.68	1153.22	1102.29
4	1084.72	1020.13	1047.65	1149.24	1059.80
5	1086.11	1029.69	1059.56	1141.58	1063.81
6	1061.32	1028.31	1047.28	1144.82	1045.76
7	1061.16	1038.96	1051.52	1115.39	1046.77
8	1052.25	1016.23	1054.90	1121.77	1071.11
9	1053.04	1024.06	1039.69	1144.90	1074.81
10	1063.98	1030.09	1055.04	1138.88	1080.74
11	1054.50	1029.37	1059.37	1136.29	1077.51
12	1042.48	1023.97	1053.04	1137.37	1076.14
13		1029.72	1055.38		1074.03
14		1028.94	1054.87		1058.27
15					1072.97
			Integration Results Adjusted for Satellite of Carbon g Overlapping with Carbon c		
1	1086.83	1028.37	1047.16	1142.03	1057.578
2	1085.15	1036.84	1060.62	1135.64	1049.773
3	1063.17	1028.24	1055.86	1153.22	1102.293
4	1096.33	1031.04	1058.86	1149.24	1059.802
5	1097.74	1040.71	1070.90	1141.58	1063.808
6	1072.67	1039.32	1058.49	1144.82	1045.763
7	1072.52	1050.07	1062.77	1115.39	1046.774
8	1063.51	1027.10	1066.19	1121.77	1071.112
9	1064.31	1035.02	1039.69	1144.90	1074.811
10	1075.37	1041.11	1055.04	1138.88	1080.744
11	1065.78	1040.38	1059.37	1136.29	1077.512
12	1053.63	1034.93	1053.04	1137.37	1076.137
13		1040.74	1055.38		1074.031
14		1039.95	1054.87		1069.59
15					1084.45
average	1074.75	1036.70	1057.02	1138.43	1068.95
std. deviation	14.0	6.4	7.6	10.7	15.4
Nominal KIE	1.075	1.037	1.057	1.138	1.069
95% confidence	0.009	0.004	0.004	0.007	0.009

Table S2 shows data from a limited study of the alternative atom pairings *a* versus *c* and *b* versus *c*. Based on our original protocol for obtaining intramolecular KIEs by NMR (reference 8a in the main text), the exploration of a different pairing required new sets of spectra with each centered on the peaks of interest. These results are consistent with the large KIEs seen in the *d* / *c* measurements and consistent with the statistical predictions for the acetophenone KIEs. As was true of the *d* / *c* results, this supports the conventional mechanism involving structures **2** through **7** and the approximate accuracy of the computational energy surface. The results for a / c and b / c are not completely independent of the results for *d* / *c* since all depend on the integration of *c*, albeit in separate sets of spectra. However, it should be noted that the large KIEs cannot be the result of an impurity under *c* since this would decrease the measured KIEs.

Table S2. Intramolecular KIE Results for **7** obtained from Di-π-methane rearrangement for other carbon pairs.

sensitizer	acetophenone	acetophenone
temperature	200 K	200 K
carbon pair	a / c	b / c
entry	Raw Integration Results	
1	1130.499	1121.897
2	1127.635	1097.316
3	1132.455	1098.161
4	1129.099	1089.346
5	1124.03	1095.864
6	1137.271	1097.538
7	1131.205	1105.697
8	1136.77	1107.238
9	1137.198	1100.674
10	1140.05	1098.05
11	1133.962	1120.465
12	1127.426	1108.488
average	1132.30	1103.39
std. deviation	4.7	9.4
Nominal KIE	1.132	1.103
95% confidence	0.003	0.005
CVT/SCT-predicted	1.124[a] 1.108[b] 1.141[c]	1.113[a] 1.105[b] 1.141[c]

[a]Calculated using the method of main text reference 7. [b]VTST-ISPE using CASSCF(6,6)+NEVPT2/aug-cc-pVTZ energies along the ω-B97XD/6-31+G** path. [c]Using LC-mPWLYP/6-31+G** calculations.

Calculation of KIEs and Errors

The isotope effects were calculated from the average adjusted integrations divided by the 1000 value assigned to carbon c. The 95% confidence ranges were calculated from the standard deviations and number of measurements in a normal way (See: http://www.iupac.org/publications/analytical_compendium/Cha02sec3.pdf).

Special Topic Discussions

The Triplet Energy Surface in the Area of 2 and Its Rearrangement Transition States.

Consideration of the theoretical methods validation studies in a later section may be aided by a detailed examination of the energy surface in the area of **2**. We will refer to five structures, though not all five are stationary points in all computational methods. The five structures are:

- **anti-2**, in which the carbons of the excited olefin are pyramidalized and the hydrogens of the pyramidalized carbons are displaced away from each other
- **syn-2**, in which the hydrogens on the pyramidalized carbons are approximately eclipsed
- **anti-synTS**, the TS for interconversion of **anti-2** and **syn-2**
- **anti-TS 3**‡, the TS that connects **anti-2** to intermediate **4**
- **syn-TS 3**‡, the TS that connects **syn-2** to intermediate **4**

We also located additional structures in this area, including an analog of **syn-2, benzo-syn-2**, with the hydrogens pointing toward the benzene ring, a TS for the formation of **benzo-syn-2**, a TS for a rearrangement involving initial bond formation at the benzene ring, and an unusual TS that accomplishes a front-to-back interconversion of **4**, but these structures were higher in energy and were judged to not be chemically relevant.

The various DFT and *ab initio* computational methods might be described as predicting *crudely* similar energy surfaces, in that all methods predict that **anti-2** is lowest in energy of the five, and most predict the relative energy of the other four structures versus **anti-2** within a range of ± 2 kcal/mol. However, the surfaces differ *qualitatively* from the perspective that some predict that the lowest barrier from **anti-2** to **4** is via **anti-TS 3**‡ (CASSCF(6,6)+NEVPT2/aug-cc-pVTZ, LC-wHPBE, LC-mPWLYP, LC-BLYP), some predict that the lowest barrier from **anti-2** to **4** is via **syn-TS 3**‡ (most DFT methods), some predict that the lowest barrier from **anti-2** to **4** is via **anti-synTS** (notably DLPNO-CCSD(T)/aug-CC-pVTZ, though this TS is importantly not consistent with the large experimental ^{13}C KIEs), and some have a single barrier along the syn pathway (the CASSCF(6,6)+NEVPT2/aug-cc-pVTZ energies look this way approximately, though this is unavoidably based on single-point energies instead of a full energy surface search) The variation in possibilities is illustrated diagrammatically in Figure S3.

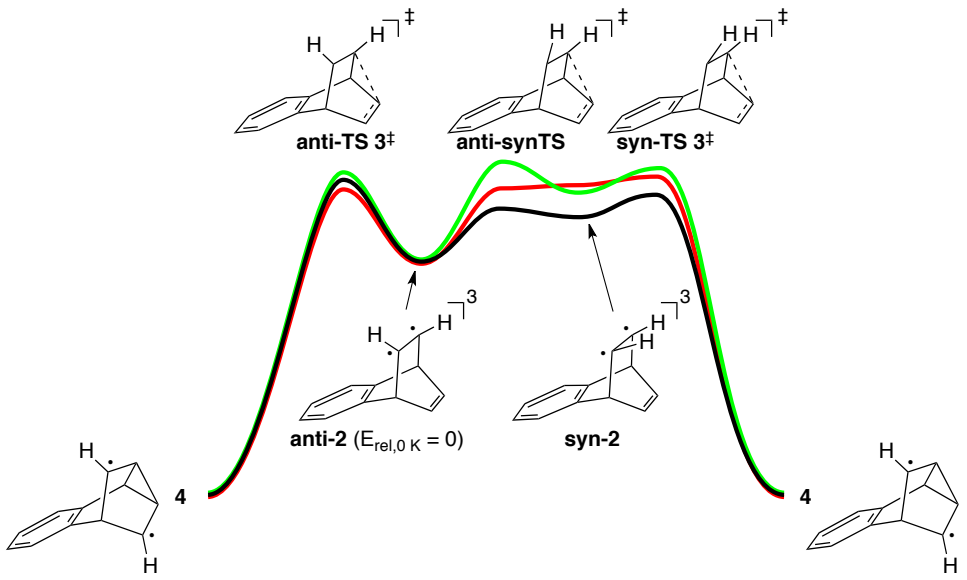

Figure S3. Diagramatic illustration, not to scale, of the variation in the energy surfaces in the area of **2** for various computational methods. The CASSCF+NEVPT2, ω-B97XD, and LC-mPWLYP surfaces are illustrated qualitatively by the red, black, and green curves, respectively.

Figure S4 shows the TD-DFT (ω-B97XD/6-31+G**) vertical excitation energy along the reaction coordinate for the reaction of **anti-2** via either **anti-TS 3**‡ or **syn-TS 3**‡. The excitation energies are large throughout, but they dip particularly of **syn-TS 3**‡ to less than 50 kcal/mol, which is where the CASSCF+NEVPT2 energies disagree modestly with the DFT energies.

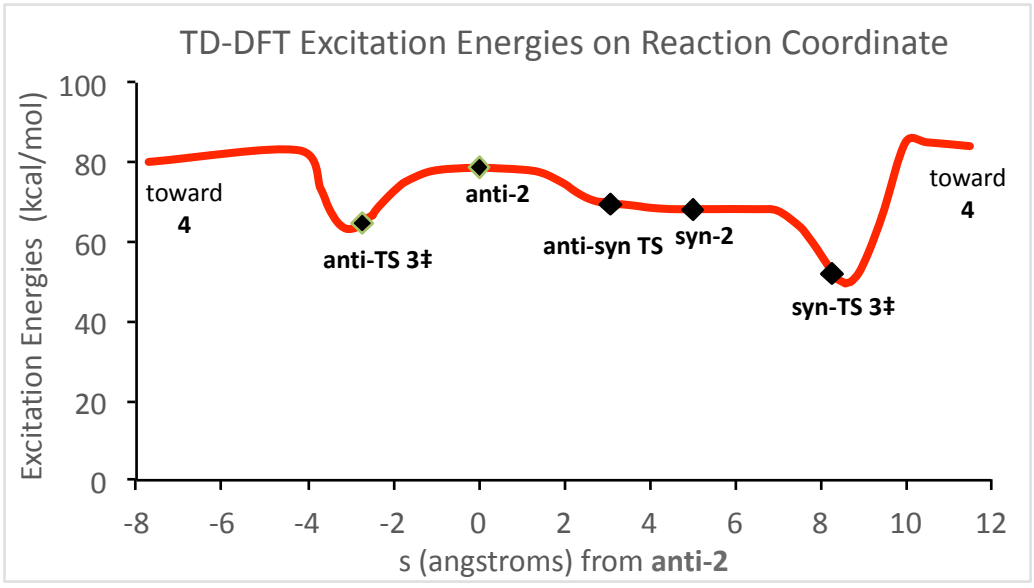

Figure S4. A connected plot of the TD-DFT (ω-B97XD/6-31+G**) vertical excitation energies along the POLYRATE / GAUSSRATE minimum energy paths through the three TSs .

Two issues add further to the complexity of understanding this surface. The first is that the zero-point energy (ZPE) along the pathway through **anti-TS 3**‡ is lower than that along the pathway through **syn-TS 3**‡, because the olefinic C-H bending vibrations are less constrained in the anti structures. ZPE thus favors the anti process by about ~0.6 kcal/mol. The second is that

tunneling adds significantly to the rate of passage through **anti-TS 3**‡ (by a factor of ~1.6 at 300 K and ~3 at 200 K) and substantially favors **anti-TS 3**‡, because the barrier though **anti-TS 3**‡ is sharper.

These issues potentially affect the detailed accuracy of the trajectory simulations. Quasiclassical trajectories reflect zero-point energy surfaces at short times (Bonnet, L. Int. Rev. Phys. Chem. 2013, 32, 171−228) but do not reflect tunneling. In addition, the ω-B97XD/6-31+G** surface has a lower barrier along the syn pathway when compared to the CASSCF(6,6)+NEVPT2/aug-cc-pVTZ (the relative energies of **anti-TS 3**‡ versus **syn-TS 3**‡ change by 0.6 kcal/mol in going from CASSCF(6,6)+NEVPT2 to ω-B97XD, favoring the syn). These factors were however considered to be sufficiently minor to allow a qualitative examination of the ω-B97XD/6-31+G** trajectories.

Comment on Main Text Reference 7

We note briefly that the Chung paper (main text reference 7) had based its predictions of exceptional heavy-atom tunneling on transition state **anti-TS 3**‡. However, the apparently unfound **syn-TS 3**‡ was actually the lowest-energy transition state for their M06-2X surface. Because the tunneling contribution to the rate for **syn-TS 3**‡ is much smaller (this is because the 'floor' for tunneling is the higher-energy **syn-2** structure), this surface if correct would lead to substantially lower tunneling. However, the CASSCF(6,6)+NEVPT2/aug-cc-pVTZ and our experimental KIEs with acetophenone support that **anti-TS 3**‡ is actually the preferred transition state and that heavy-atom tunneling through this transition state is substantial, and in this way the general conclusion of the Chung paper is supported qualitatively.

Comment on a Prior Proposed Effect of Triplet Sensitizers Providing Vibrational Energy

As cited in main text reference 4b, in 2005 Armesto, Ortiz, Agarrabeitia, and El-Boulifi reported an intriguing apparent effect of sensitizer energy on the oxa-di-π-methane rearrangement. In the sensitized reaction of β-γ-unsaturated methyl ketone **S1**, only starting material was obtained when the reaction was carried out with acetophenone (E_T = 73 kcal/mol). However, only the oxa-di-π-methane product **S2** was formed when thioxanthone (E_T = 63 kcal/mol) was the sensitizer. Lower-energy sensitizers provide more and then exclusively the 1,3-rearrangement product **S3**.

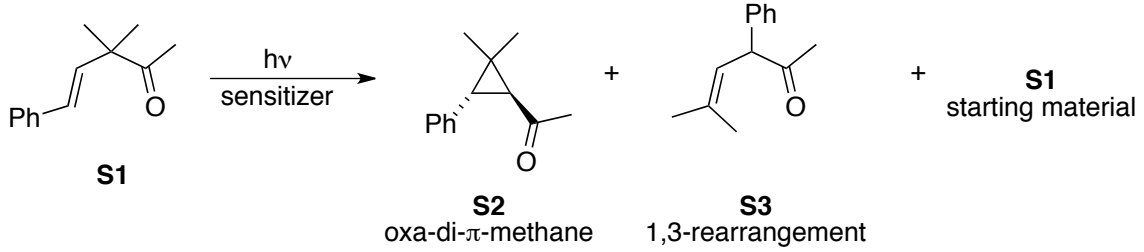

	E_T			
acetophenone	73	--	--	91%
thioxanthone	63	50%	--	20%
4-phenylbenzophenone	61	10%	28%	35%
chrysene	57	--	6%	56%

It was proposed in this first paper that acetophenone gave rise to '*"hot" triplet excited states,*

with a large excess of vibrational energy' that deactivated 'by E/Z isomerization exclusively' while '*"warm" triplet excited states*' gave rise to the oxa-di-π-methane rearrangement and '*"cold" triplet excited states*' apparently give rise to the 1,3-rearrangement.

In a later paper (also in main text reference 4b), the authors appear to walk away from this explanation based on studies of the di-π-methane reaction of structures of type **S4**: "Although our previous studies with related unsaturated ketones suggested that a possible correlation exists between the triplet energy of the sensitizer and the photoreactivity observed, the observations made in this study demonstrate that this correlation does not apply to dienes 4. Therefore, other factors (still unknown) must play an important role in the outcome of triplet-sensitized reactions of acyclic 1,4-dienes." No mention of vibrational energy or "hot" triplets appears in this paper. The authors had, as with **S1**, observed a degree of sensitizer-dependent results but these results were apparently not viewed as congruent with the hot and cold triplet idea above. A notable observation was that the reaction of **S4**, R=Ph, R'=R"=Me, saw improved yields when the E_T was both increased and decreased from that of benzophenone.

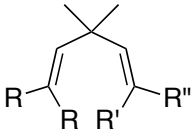

S4

In a third paper (Armesto, D.; Ortiz, M. J.; Agarrabeitia, A. R.; El-Boulifi, N. Efficient photochemical synthesis of 2-vinylcyclopropanecarbaldehydes, precursors of cyclopropane components present in pyrethroids, by using the oxa-di-p-methane rearrangement. *Tetrahedron* **2010**, *66*, 8690-8697.), Armesto and Ortiz observed sensitizer-dependent chemistry in competition between the oxa-di-π-methane reaction of **S5** to afford **S6** and its decarbonylation forming **S7** (or isomers). The key observation was that the decarbonylation reaction was observed with a high-energy sensitizer (3-methoxyacetophenone, E_T = 71 kcal/mol) but not with a low-energy triplet sensitizer (4-phenylbenzophenone, E_T = 61 kcal/mol).

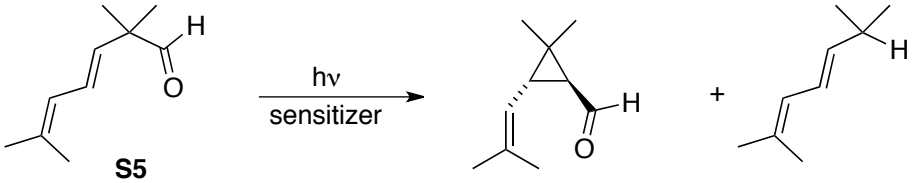

S5 **S6** oxa-di-π-methane **S7** decarbonylation only observed with high-energy sensitizer

Of the systems studied in the three papers, we view the results with **S5** as most interesting because they fit with chemical intuition and a potentially straightforward physical explanation of the results in terms of the involvement of a "hot" triplet. The authors themselves at this point no longer referred to either the idea of hot triplets nor to any role for excess vibrational energy, but in the reactions of **S5**, the possibility that decarbonylation is promoted by vibrational excitation of the triplet **S5** on formation seems at least physically plausible and worth future exploration. In contrast, bluntly, we could not discern any simple physical explanation for the results with **S1** and **S4** that would relate vibrational excitation to the experimental observations. The complete lack of oxa-di-π-methane product from **S1** with the highest-energy sensitizer seems particularly difficult to ascribe to a vibrationally activated intermediate.

In all of these systems, a number of potential complications and study limitations hamper the interpretation of the results. At one level, a more quantitative approach than the simple

reporting of yields after a set irradiation time would have aided in the analysis of the data. On a different level, a substantial issue is that these acyclic structures are conformationally rich. The singlet ground state of **S1** has three available conformations within 0.5 kcal/mol (ω-B97XD/6-31+G**) and these can give rise to a total of four conformations of the triplet of **S1**, **S8 – S11**. Considering that the conventional explanation of triplet sensitizer-dependent chemistry is the formation of differing mixtures of excited state conformers (see reference 4a in the main text), it is surprising that this issue was apparently not considered in the original work. (One advantage in the choice of benzobarrelene in the current study was the absence of the complication of multiple ground-state conformations.)

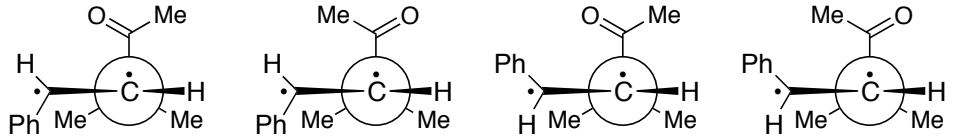

S8 **S9** **S10** **S11**

Overall, it remains possible that the work of Armesto and Ortiz exhibits the effects of vibrationally excited triplets due to varying sensitizer energies seen in the current paper, but the series of papers on this issue ended up with the authors no longer asserting this, and further work would be required to assess the proposal.

The Triplet Energy of Benzobarrelene.

As described in reference 16 of the main text, Zimmerman, Amick, and Hemetsberger (Zimmerman, H. E.; Amick, D. R.;; Hemetsberger, H. Photochemical Rearrangement Effected by Triplet Excitation Transmitted through a High Energy Moiety. *J. Am. Chem. Soc.* **1973**, *95*, 4606-4610) had reported a triplet energy for benzobarrelene of 79.3 kcal/mol. This is based on the phosphorescence spectrum, as described in the thesis of one of the authors (Amick, D. R. "Aromatic Barrelene Rearrangements." University of Wisconsin, 1972, pp 88) without experimental details. From experiments alone, this value would be very surprising since acetophenone (E_T = 73.3 kcal/mol) is a highly efficient sensitizer for the reaction (Φ ~ 0.5). In addition, in the similar dibenzobarrelene case acetone (E_T = 81.2 kcal/mol) and acetophenone transfer their energy at nearly identical rates (see main text reference 14). (We note that it is experimentally difficult to obtain benzobarrelene in analytically pure form, and impurities are a conventional source of error in phosphorescence spectra. The absence of experimental details makes this possibility difficult to assess.)

Computationally, the E_T predicted from a series of *ab initio* composite methods in addition to DLPNO-CCSD(T)/aug-cc-pVTZ//ω-B97XD/6-31+G** calculations is show in Table S3. The range of results from these methods is notably large, but all fall much lower than the reported value. It should be noted that these composite methods are highly accurate in their prediction of E_T for acetone (G3 and G3B3 methods find 81.2 and 80.9 kcal/mol, compared to the experimental 81.2 kcal/mol.

For the work in the main text, we have taken the E_T as being ~69 kcal/mol, in line with the lowest-energy sensitizer that promotes the reaction and the average of the computational values. However, a range of E_T's within ±3 kcal/mol of this value would make no meaningful difference in the results. For example, the predicted RRKM KIE at a vibrational energy of 10.0 kcal/mol in place of the 13.0 kcal/mol value used in the main text changes to 1.033 from the original 1.031.

Table S3. Energies of Singlet and Triplet Benzobarrelene from *ab initio* Methods.

Method	multiplicity	E + zpe	E(T)
G1	singlet	-462.350615	
	triplet	-462.234776	72.7
G2	singlet	-462.349055	
	triplet	-462.23463	71.8
G2MP2	singlet	-462.340566	
	triplet	-462.225783	72.0
G3	singlet	-462.889516	
	triplet	-462.778494	69.7
G3B3	singlet	-462.900046	
	triplet	-462.791075	68.4
G3MP2	singlet	-462.441296	
	triplet	-462.329397	70.2
G4	singlet	-462.973157	
	triplet	-462.867682	66.2
G4MP2	singlet	-462.494014	
	triplet	-462.388515	66.2
DLPNO-CCSD(T)/aug-cc-pVTZ	singlet	-462.217392	
+ zpe from ω-B97XD/6-31+G**	triplet	-462.110365	67.2

Computational Procedures and Results

General Procedures

The calculations of DFT or MP2 structures, energies, and frequencies employed default procedures in Gaussian16[3] unless otherwise noted. CASSCF+NEVPT2 and DLPNO-CCSD(T) energies were calculated using ORCA 4.0.1.[4] Calculations of KIEs including small-curvature tunneling (SCT) employed the GAUSSRATE / POLYRATE set of programs.[5,6] Complete structures and energetics are provided in sections below, as well as additional details on the calculations and relevant program input files. All absolute energies are in Hartrees. All relative energies are presented in kcal/mol.

Calculations of trajectories employed the program suite PROGDYN. PROGDYN consists of a series of component programs written as either Unix shell scripts or awk programs. Gaussian16 was used to calculate the forces at each point in trajectories. A detailed description of PROGDYN's subprograms, inputs and outputs can be found in the Supporting Information for a recent paper ("Solvation Dynamics and the Nature of Reaction Barriers and Ion-Pair Intermediates in Carbocation Reactions," Roytman, V. A.; Singleton, D. A. *J. Am. Chem. Soc.* **2020**, *142*, 12865-12877. DOI: 10.1021/jacs.0c06295). A full listing of the subprograms of PROGDYN can be found as a permanent public dataverse set at https://dataverse.harvard.edu/dataset.xhtml?persistentId=doi:10.7910/DVN/TQZR7E. A later

section contains PROGDYN usage details and configuration parameters.

The authors request that users of these programs inform them at singleton@chem.tamu.edu for notifications of bug fixes and updated features and to allow tracking of the broader impacts of the programs.

Calculations of KIEs based on RRKM microcanonical rate constants made use of the QCPE RRKM program. A complete description of the theory and parameters used in the program can be found in https://cdssim.chem.ttu.edu/RRKM/Doc/RRKM_manual.pdf.

A diverse collection of short helper and data-analysis programs were used to aid the running of trajectories and to analyze the data. A later section describes the general purpose, input, and output of each of these programs. A full listing of each can be found in a separate Supporting Information zip file.

Computational Methods Validation Studies

To explore the accuracy of computational methods for the di-π-methane rearrangement, a series of structures were first optimized in gas-phase unrestricted ωB97XD/6-31+G(d,p) calculations. Single-point energies for each of these structures were then calculated in DLPNO-CCSD(T)/aug-cc-pVTZ calculations, and the energetics were then calculated in a series of DFT calculations, as shown in Table S4 and S5. The ωB97xD/6-31+G(d,p) was chosen as the working optimization method based on it being closest to getting the relative energy of **anti-TS 3**‡ versus **anti-2** compared to the DLPNO-CCSD(T) calculation. As the course of the research evolved we opted to prefer the use of the CASSCF+NEVPT2/aug-cc-pVTZ calculations as a primary standard, but the ωB97xD/6-31+G(d,p) remained a good choice by this measure.

The LC-mPWLYP/6-31+G** calculations require some particular comment. As we note in a previous section, the CASSCF+NEVPT2/aug-cc-pVTZ calculations predict that the lowest barrier from **anti-2** to **4** is via **anti-TS 3**‡. This was true of LC DFT methods, though most DFT calculations predict the opposite (Table S5). Because the LC-mPWLYP/6-31+G** calculations get this aspect of the surface right, we explored them in more detail and carried out KIE calculations with them. Those are retained for the main text, but the LC-mPWLYP/6-31+G** calculations appear to overestimate the barrier for **anti-TS 3**‡ leading to an overestimate of tunneling and the predicted KIE.

There is little polarity in **anti-2**; its B3LYP/6-31+G** dipole moment is within 2% of that for **1**, and the barrier ω-B97XD/6-31+G** barrier for passing over **anti-TS 3**‡ was decreased by only 0.1 kcal/mol employing a PCM solvent model.

Table S4. DFT methods exploration based on anti-TS 3‡. All structures are based on ω-B97XD/6-31+G** optimized structures

Method	Basis set	anti-2	anti-TS 3‡	ΔE (kcal/mol)
DLPNO-CCSD(T)	aug-cc-pVTZ	-462.2902453	-462.2834899	4.2
M062X	6-31+G*	-462.9354833	-462.9259711	6.0
M062X	6-311+G**	-463.0541951	-463.0456957	5.3
B3LYP	6-311+G**	-463.2535836	-463.2481255	3.4
ωB97xD	6-31+G**	-462.2906565	-462.2839465	4.2
ωB97xD	6-311+G**	-463.0916214	-463.085059	4.1
B3PW91	6-311+G**	-463.0768334	-463.0728114	2.5
mPW-PW91	6-311+G**	-463.1862855	-463.1850827	0.8

mPW1PW91	6-311+G**	-463.1495836	-463.1450156	2.9
TPSSTPSS	6-311+G**	-463.3428364	-463.3402876	1.6
X3LYP	6-311+G**	-463.0256911	-463.0200753	3.5
BMK	6-311+G**	-462.9172207	-462.9127703	2.8
CAM-B3LYP	6-311+G**	-462.9820031	-462.9744447	4.7
PBE-PBE	6-311+G**	-462.6482521	-462.6476336	0.4
HSEH1PBE	6-311+G**	-462.7402267	-462.735966	2.7
B-VP86	6-311+G**	-463.2710588	-463.2696253	0.9
APFD	6-311+G**	-462.8700168	-462.8658807	2.6
HCTH407	6-311+G**	-463.1904571	-463.1889651	0.9
S-VWN	6-311+G**	-460.590683	-460.5945364	-2.4
TPSSh	6-311+G**	-463.2957222	-463.2920062	2.3
LC-wPBE	6-311+G**	-462.9151693	-462.9072067	5.0
B3P86	6-311+G**	-464.7332953	-464.7295526	2.3
HISSbPBE	6-311+G**	-462.7264665	-462.72017	4.0
tHCTHhyb	6-311+G**	-463.1768547	-463.1733083	2.2

Table S5. DFT methods exploration of syn-TS 3‡. All structures are based on ω-B97XD/6-31+G** optimized structures

Method	Basis set	syn-TS 3‡	anti-TS 3‡	ΔE (kcal/mol)
DLPNO-CCSD(T)	aug-cc-pVTZ	**-462.2902453**	**-462.2834899**	4.2
ω-B97XD	6-31+G**	-463.0081911	-463.006917	0.8
M062X	6-31+G**	-462.954579	-462.9540112	0.4
B3LYP	6-31+G**	-463.1693071	-463.1660178	2.1
HSEH1PBE	6-31+G**	-462.6621335	-462.6601135	1.3
OHSE2PBE	6-31+G**	-463.5415243	-463.5395733	1.2
OHSE1PBE	6-31+G**	-462.6630647	-462.6610457	1.3
LC-wPBE	6-31+G**	-462.8286308	-462.8303456	-1.1
CAM-B3LYP	6-31+G**	-462.8920554	-462.890931	0.7
M11	6-31+G**	-462.8535767	-462.853886	-0.2
N12SX	6-31+G**	-462.970874	-462.9687706	1.3
MN12SX	6-31+G**	-462.7851532	-462.7821505	1.9
B3P86	6-31+G**	-464.6520775	-464.6493496	1.7
B3PW91	6-31+G**	-462.9972218	-462.9946935	1.6
B1B95	6-31+G**	-462.9529615	-462.9500972	1.8
mPW1PW91	6-31+G**	-463.0698308	-463.0679586	1.2
mPW1LYP	6-31+G**	-462.9044088	-462.9015957	1.8
mPW1PBE	6-31+G**	-462.8900084	-462.8881733	1.2
mPW3PBE	6-31+G**	-462.8480855	-462.8455462	1.6
B98	6-31+G**	-462.9762579	-462.9731419	2.0
B971	6-31+G**	-463.0335345	-463.0302556	2.1
B972	6-31+G**	-463.0071533	-463.0039882	2.0
PBE1PBE	6-31+G**	-462.6241662	-462.62224	1.2
LC-wHPBE	6-31+G**	-462.8275208	-462.8292353	-1.1
MN15	6-31+G**	-462.5907851	-462.5882483	1.6
PBE0	6-31+G**	-462.6230102	-462.6230102	0.0
BMK	6-31+G**	-462.836914	-462.8344204	1.6
LC-mPWLYP	6-31+G**	-461.7209061	-461.722286	-0.9
LC-UBLYP	6-31+G**	-461.714446	-461.7158307	-0.9
LC-BRxPL	6-31+G**	-464.0770462	-464.0783319	-0.8

KIE Calculations from POLYRATE Data

The qualitative mechanism for the benzobarrelene di-π-methane rearrangement is illustrated in Scheme S1 with the carbons labeled. The POLYRATE rate constants for non-labeled as well as ^{13}C-labelled at each position from a to d are summarized in Tables S6 and S7. The calculation of the product isotopic distribution from these rate constants requires a choice between three differing plausible assumptions. We refer to these assumptions as "non-Curtin-Hammett," "partial Curtin-Hammett", and "full Curtin-Hammett."

As noted in the main text, the structure of **2** is not symmetrical due to its pyramidalized radical centers. At the extreme of the "non-Curtin-Hammett" assumption, these non-equivalent

centers do not exchange and react inequivalently, so that the choice of which center reacts would be decided by the initial asymmetry adopted by **2** on excitation. (We assume in every case that the choice of which alkene is excited and the initial pyramidalization of the carbons for this alkene are subject to negligible KIEs.) If this were the case, there would be no significant isotope effect for the first step (bond making) of the mechanism. The overall observed isotope effects would be much lower than those experimentally observed with acetophenone (~1.03 at 300 K, ~1.07 at 200 K) since they would arise only from the KIE for the second step. The non-Curtin-Hammett assumption is then inconsistent with the experimental observations.

At the opposite extreme, the full Curtin-Hammett assumption would be that the pyramidal centers of **2** rapidly interconvert and that the excitation can move rapidly between the two olefinic centers. With this assumption, the fraction of ^{13}C in the original olefins that ends up in the a and d positions of **4** is:

labeled at a/d in **4** = $(r_{a1} + r_{d1}) / (r_{a1} + r_{b1} + r_{c1} + r_{d1})$ (S1)

while at b and c of **4** is:

labeled at b/c in **4** = $(r_{b1} + r_{c1}) / (r_{a1} + r_{b1} + r_{c1} + r_{d1})$ (S2)

where "*r*" is a calculated rate constant; *a*, *b*, *c*, and *d* refer to the positions of the ^{13}C in Scheme S1, and *1* or *2* refer to first step (**2** to **4**) versus second (bond breaking) step (**4** to **6**) in the mechanism.

For the second step the ^{13}C in a/d of **4** is partitioned to **6** and ultimately to **7** as:

label at a of **6**/**7** = (labeled at a/d in **4**) × $(r_{a2} / (r_{a2} + r_{d2}))$ (S3)

label at d of **6**/**7** = (labeled at a/d in **4**) × $(r_{d2} / (r_{a2} + r_{d2}))$ (S4)

and the ^{13}C in b/c of **4** is partitioned to **6** and ultimately to **7** as:

label at b of **6**/**7** = (labeled at b/c in **4**) × $(r_{b2} / (r_{b2} + r_{c2}))$ (S5)

label at c of **6**/**7** = (labeled at b/c in **4**) × $(r_{c2} / (r_{b2} + r_{c2}))$ (S6)

The reported nominal KIEs in Tables S8 and S9 and the main text are then the ratio of (label at d) / (label at c) from eqs S4 and S6 above.

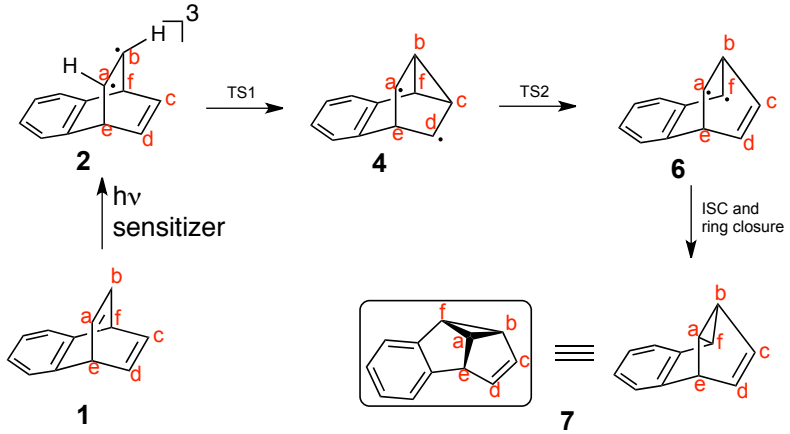

Scheme S1. Reaction scheme for the benzobarrelene di-π-methane rearrangement and carbon assignment

The "partial Curtin-Hammett" assumption is that the pyramidal centers rapidly interconvert but that the excitation does not move rapidly between the two olefinic centers. If this is the case, then by an analogous process to that above, the label in the various carbons would be

defined by eqs S7 to S10.

$$\text{label at a of } \mathbf{6}/\mathbf{7} = \left(\frac{r_{b1}}{r_{a1}+r_{b1}}+\frac{r_{c1}}{r_{c1}+r_{d1}}\right)\left(\frac{r_{d2}}{r_{a2}+r_{d2}}\right) \quad \text{(S7)}$$

$$\text{label at b of } \mathbf{6}/\mathbf{7} = \left(\frac{r_{a1}}{r_{a1}+r_{b1}}+\frac{r_{d1}}{r_{c1}+r_{d1}}\right)\left(\frac{r_{c2}}{r_{b2}+r_{c2}}\right) \quad \text{(S8)}$$

$$\text{label at c of } \mathbf{6}/\mathbf{7} = \left(\frac{r_{a1}}{r_{a1}+r_{b1}}+\frac{r_{d1}}{r_{c1}+r_{d1}}\right)\left(\frac{r_{b2}}{r_{b2}+r_{c2}}\right) \quad \text{(S9)}$$

$$\text{label at d of } \mathbf{6}/\mathbf{7} = \left(\frac{r_{b1}}{r_{a1}+r_{b1}}+\frac{r_{c1}}{r_{c1}+r_{d1}}\right)\left(\frac{r_{a2}}{r_{a2}+r_{d2}}\right) \quad \text{(S10)}$$

The results from S7 to S10 are extremely close to those from S1 to S6, being consistently slightly smaller but never differing by more than 0.001 at 300 K and 0.003 at 200K. We cannot experimentally distinguish the full Curtin-Hammett and partial Curtin-Hammett possibilities, but the difference is not relevant to the conclusions of the paper.

Multireference character was judged to be of less importance to second step in the mechanism, and the full-path CASSCF calculations for the ISPE calculations in POLYRATE were not carried out. Instead, the first-step CASSCF rate constants were combined with ω-B97XD second-step rate constants for the purpose of isotope effect predictions.

Numerical convergence can be difficult to achieve for the calculation of small isotope effects by this method, and POLYRATE's SSTEP parameter is the key factor. (Other factors contributing to numerical non-convergence are more easily controlled, while calculations with a small SSTEP are costly.) The calculations with differing SSTEP values were carried out to gauge the potential errors due to a lack of numerical convergence, and it appears that the errors are small, 0.004 at 200 K and 0.002 at 300 K.

Table S6. POLYRATE rate constants (200 K)

^{13}C position	no label					
Method	**Step**	**SSTEP**	**TST**	**CVT**	**TST/SCT**	**CVT/SCT**
M06-2X	Bond-forming	0.01	3.1691E+07	2.9618E+07	9.9549E+07	1.0053E+08
ωB97xD	Bond-forming	0.01	5.9521E+09	5.7173E+09	1.3065E+10	1.2920E+10
ωB97xD	Bond-forming	0.005	5.9521E+09	5.7204E+09	1.2861E+10	1.2722E+10
ωB97xD	Bond-forming	0.0025	5.9521E+09	5.7206E+09	1.2714E+10	1.2577E+10
ωB97xD CAS-ISPE	Bond-forming	0.0025	6.6449E+09	6.5444E+09	8.8883E+09	2.0640E+10
LC-mPWLYP	Bond-forming	0.01	5.8533E+07	5.8341E+07	2.0215E+08	2.0242E+08
M06-2X	Bond-breaking	0.01	5.4460E+02	5.2793E+02	1.4791E+03	1.4788E+03
ωB97xD	Bond-breaking	0.01	3.3390E+04	3.3381E+04	8.8258E+04	8.8290E+04
LC-mPWLYP	Bond-breaking	0.01	4.9995E+00	4.9957E+00	2.2184E+01	2.2168E+01

^{13}C position	a					
Method	**Step**	**SSTEP**	**TST**	**CVT**	**TST/SCT**	**CVT/SCT**
M06-2X	Bond-forming	0.01	3.1801E+07	2.9712E+07	9.9857E+07	1.0085E+08
ωB97xD	Bond-forming	0.01	5.9673E+09	5.7296E+09	1.3109E+10	1.2964E+10
ωB97xD	Bond-forming	0.005	5.9673E+09	5.7327E+09	1.2906E+10	1.2766E+10
ωB97xD	Bond-forming	0.0025	5.9673E+09	5.7329E+09	1.2772E+10	1.2633E+10
ωB97xD CAS-ISPE	Bond-forming	0.0025	7.4814E+09	7.4008E+09	1.0735E+10	2.2447E+10
LC-mPWLYP	Bond-forming	0.01	5.8781E+07	5.8582E+07	2.0246E+08	2.0274E+08

M06-2X	Bond-breaking	0.01	5.4514E+02	5.2854E+02	1.4804E+03	1.4800E+03
ωB97xD	Bond-breaking	0.01	3.3442E+04	3.3434E+04	8.8365E+04	8.8397E+04
LC-mPWLYP	Bond-breaking	0.01	5.0114E+00	5.0075E+00	2.2226E+01	2.2211E+01

^{13}C position b

Method	Step	SSTEP	TST	CVT	TST/SCT	CVT/SCT
M06-2X	Bond-forming	0.01	3.0848E+07	2.8740E+07	9.1536E+07	9.2547E+07
ωB97xD	Bond-forming	0.01	5.8033E+09	5.5626E+09	1.2383E+10	1.2240E+10
ωB97xD	Bond-forming	0.005	5.8033E+09	5.5656E+09	1.2126E+10	1.1989E+10
ωB97xD	Bond-forming	0.0025	5.8033E+09	5.5658E+09	1.2010E+10	1.1875E+10
ωB97xD CAS-ISPE	Bond-forming	0.0025	7.3118E+09	7.2355E+09	1.0211E+10	2.1241E+10
LC-mPWLYP	Bond-forming	0.01	5.6944E+07	5.6734E+07	1.8645E+08	1.8672E+08
M06-2X	Bond-breaking	0.01	5.5175E+02	5.3511E+02	1.4872E+03	1.4866E+03
ωB97xD	Bond-breaking	0.01	3.3974E+04	3.3968E+04	8.9080E+04	8.9108E+04
LC-mPWLYP	Bond-breaking	0.01	5.0732E+00	5.0689E+00	2.2242E+01	2.2226E+01

^{13}C position c

Method	Step	SSTEP	TST	CVT	TST/SCT	CVT/SCT
M06-2X	Bond-forming	0.01	3.0414E+07	2.8410E+07	9.2003E+07	9.2954E+07
ωB97xD	Bond-forming	0.01	5.7263E+09	5.4988E+09	1.2291E+10	1.2152E+10
ωB97xD	Bond-forming	0.005	5.7263E+09	5.5017E+09	1.2095E+10	1.1961E+10
ωB97xD	Bond-forming	0.0025	5.7263E+09	5.5019E+09	1.1947E+10	1.1814E+10
ωB97xD CAS-ISPE	Bond-forming	0.0025	7.3789E+09	7.2769E+09	1.0119E+10	2.0555E+10
LC-mPWLYP	Bond-forming	0.01	5.5996E+07	5.5819E+07	1.8564E+08	1.8589E+08
M06-2X	Bond-breaking	0.01	5.1469E+02	4.9881E+02	1.3352E+03	1.3356E+03
ωB97xD	Bond-breaking	0.01	3.1755E+04	3.1748E+04	8.0748E+04	8.0777E+04
LC-mPWLYP	Bond-breaking	0.01	4.7058E+00	4.7019E+00	1.9489E+01	1.9475E+01

^{13}C position d

Method	Step	SSTEP	TST	CVT	TST/SCT	CVT/SCT
M06-2X	Bond-forming	0.01	3.0942E+07	2.8984E+07	9.7104E+07	9.8007E+07
ωB97xD	Bond-forming	0.01	5.8119E+09	5.5908E+09	1.2765E+10	1.2625E+10
ωB97xD	Bond-forming	0.005	5.8119E+09	5.5938E+09	1.2561E+10	1.2426E+10
ωB97xD	Bond-forming	0.0025	5.8119E+09	5.5940E+09	1.2428E+10	1.2295E+10
ωB97xD CAS-ISPE	Bond-forming	0.0025	7.1467E+09	7.0316E+09	1.0240E+10	2.1855E+10
LC-mPWLYP	Bond-forming	0.01	5.7090E+07	5.6922E+07	1.9692E+08	1.9717E+08
M06-2X	Bond-breaking	0.01	5.5208E+02	5.3586E+02	1.5024E+03	1.5015E+03
ωB97xD	Bond-breaking	0.01	3.3845E+04	3.3839E+04	8.9583E+04	8.9611E+04
LC-mPWLYP	Bond-breaking	0.01	5.0698E+00	5.0652E+00	2.2523E+01	2.2507E+01

Table S7. POLYRATE rate constants (300 K)

^{13}C position N/A

Method	Step	Step size	TST	CVT	TST/SCT	CVT/SCT
M06-2X	Bond-forming	0.01	2.3170E+09	2.2334E+09	3.5484E+09	3.5944E+09
ωB97xD	Bond-forming	0.01	8.3485E+10	8.0466E+10	1.1509E+11	1.1287E+11
ωB97xD	Bond-forming	0.005	8.3485E+10	8.0504E+10	1.1430E+11	1.1213E+11
ωB97xD	Bond-forming	0.0025	8.3485E+10	8.0509E+10	1.1378E+11	1.1162E+11
ωB97xD CAS-ISPE	Bond-forming	0.0025	8.6894E+10	8.5795E+10	8.0056E+10	1.3996E+11
LC-mPWLYP	Bond-forming	0.01	3.3905E+09	3.3852E+09	5.5338E+09	5.5413E+09
M06-2X	Bond-breaking	0.01	1.5213E+06	1.5011E+06	2.2258E+06	2.2345E+06
ωB97xD	Bond-breaking	0.01	2.2743E+07	2.2742E+07	3.3529E+07	3.3534E+07
LC-mPWLYP	Bind-breaking	0.01	6.4808E+04	6.4740E+04	1.1375E+05	1.1360E+05

^{13}C position a

Method	Step	Step size	TST	CVT	TST/SCT	CVT/SCT
M06-2X	Bond-forming	0.01	2.3212E+09	2.2370E+09	3.5535E+09	3.5998E+09
ωB97xD	Bond-forming	0.01	8.3604E+10	8.0553E+10	1.1530E+11	1.1307E+11
ωB97xD	Bond-forming	0.005	8.3604E+10	8.0591E+10	1.1449E+11	1.1230E+11
ωB97xD	Bond-forming	0.0025	8.3604E+10	8.0596E+10	1.1399E+11	1.1183E+11
ωB97xD CAS-ISPE	Bond-forming	0.0025	9.4921E+10	9.4099E+10	9.1458E+10	1.4929E+11
LC-mPWLYP	Bond-forming	0.01	3.3980E+09	3.3926E+09	5.5407E+09	5.5484E+09
M06-2X	Bond-breaking	0.01	1.5217E+06	1.5016E+06	2.2265E+06	2.2351E+06
ωB97xD	Bond-breaking	0.01	2.2757E+07	2.2757E+07	3.3547E+07	3.3552E+07
LC-mPWLYP	Bind-breaking	0.01	6.4882E+04	6.4813E+04	1.1386E+05	1.1371E+05

^{13}C position b

Method	Step	Step size	TST	CVT	TST/SCT	CVT/SCT
M06-2X	Bond-forming	0.01	2.2686E+09	2.1827E+09	3.4008E+09	3.4485E+09
ωB97xD	Bond-forming	0.01	8.1842E+10	7.8738E+10	1.1147E+11	1.0924E+11
ωB97xD	Bond-forming	0.005	8.1842E+10	7.8775E+10	1.1049E+11	1.0831E+11
ωB97xD	Bond-forming	0.0025	8.1842E+10	7.8780E+10	1.1002E+11	1.0785E+11
ωB97xD CAS-ISPE	Bond-forming	0.0025	9.3230E+10	9.2433E+10	8.8776E+10	1.4439E+11
LC-mPWLYP	Bond-forming	0.01	3.3182E+09	3.3123E+09	5.3138E+09	5.3215E+09
M06-2X	Bond-breaking	0.01	1.5320E+06	1.5120E+06	2.2361E+06	2.2445E+06
ωB97xD	Bond-breaking	0.01	2.2964E+07	2.2963E+07	3.3757E+07	3.3761E+07
LC-mPWLYP	Bind-breaking	0.01	6.5340E+04	6.5267E+04	1.1424E+05	1.1409E+05

^{13}C position	c					
Method	**Step**	**Step size**	**TST**	**CVT**	**TST/SCT**	**CVT/SCT**
M06-2X	Bond-forming	0.01	2.2483E+09	2.1665E+09	3.3967E+09	3.4420E+09
ωB97xD	Bond-forming	0.01	8.1143E+10	7.8172E+10	1.1085E+11	1.0866E+11
ωB97xD	Bond-forming	0.005	8.1143E+10	7.8208E+10	1.1009E+11	1.0794E+11
ωB97xD	Bond-forming	0.0025	8.1143E+10	7.8212E+10	1.0949E+11	1.0736E+11
ωB97xD CAS-ISPE	Bond-forming	0.0025	9.3683E+10	9.2634E+10	8.9181E+10	1.4266E+11
LC-mPWLYP	Bond-forming	0.01	3.2829E+09	3.2780E+09	5.2802E+09	5.2872E+09
M06-2X	Bond-breaking	0.01	1.4639E+06	1.4445E+06	2.1076E+06	2.1165E+06
ωB97xD	Bond-breaking	0.01	2.1969E+07	2.1969E+07	3.1946E+07	3.1950E+07
LC-mPWLYP	Bind-breaking	0.01	6.2207E+04	6.2138E+04	1.0678E+05	1.0664E+05

^{13}C position	d					
Method	**Step**	**Step size**	**TST**	**CVT**	**TST/SCT**	**CVT/SCT**
M06-2X	Bond-forming	0.01	2.2808E+09	2.2015E+09	3.4939E+09	3.5372E+09
ωB97xD	Bond-forming	0.01	8.2196E+10	7.9309E+10	1.1337E+11	1.1121E+11
ωB97xD	Bond-forming	0.005	8.2196E+10	7.9347E+10	1.1257E+11	1.1046E+11
ωB97xD	Bond-forming	0.0025	8.2196E+10	7.9351E+10	1.1209E+11	1.0999E+11
ωB97xD CAS-ISPE	Bond-forming	0.0025	9.2203E+10	9.1100E+10	8.8441E+10	1.4640E+11
LC-mPWLYP	Bond-forming	0.01	3.3352E+09	3.3306E+09	5.4413E+09	5.4481E+09
M06-2X	Bond-breaking	0.01	1.5346E+06	1.5153E+06	2.2477E+06	2.2556E+06
ωB97xD	Bond-breaking	0.01	2.2941E+07	2.2940E+07	3.3839E+07	3.3842E+07
LC-mPWLYP	Bind-breaking	0.01	6.5388E+04	6.5312E+04	1.1480E+05	1.1465E+05

Table S8. POLYRATE KIEs (200 K)

KIE (d / c)	**SSTEP**	**TST**	**CVT**	**TST/SCT**	**CVT/SCT**
M06-2X	0.01	1.068	1.072	1.142	1.141
ωB97xD	0.01	1.064	1.066	1.110	1.111
ωB97xD	0.005	1.064	1.066	1.114	1.114
ωB97xD	0.0025	1.064	1.066	1.114	1.115
ωB97xD CAS-ISPE	0.0025	1.036	1.035	1.093	1.123
LC-mPWLYP	0.01	1.072	1.072	1.157	1.157

Table S9. POLYRATE KIEs (300 K)

KIE (d / c)	SSTEP	TST	CVT	TST/SCT	CVT/SCT
M06-2X	0.01	1.047	1.049	1.073	1.072
ωB97xD	0.01	1.044	1.046	1.062	1.063
ωB97xD	0.005	1.044	1.046	1.063	1.064
ωB97xD	0.0025	1.044	1.046	1.064	1.065
ωB97xD CAS-ISPE	0.0025	1.028	1.027	1.044	1.064
LC-mPWLYP	0.01	1.050	1.050	1.077	1.077

Location of Structure 8

As described in the main text, within the formalism of Frutos and coworkers (main text reference 19) the transition state for triplet energy transfer is the lowest-energy structure lowest-energy geometry of **1** that has an excitation energy that matches the triplet energy of the sensitizer. The Frutos work used a gradient approach to finding this structure, but the algorithm code was not available until after the work with **8** was complete. (We thank Dr. Luis Frutos for providing this code, though it was not used for the paper results.) Instead, we used a grid approach to the location of **8**. A survey of the effect of internal coordinate values on the excitation energy indicated that the key coordinates were the olefinic C-C bond distance (d_{CC} below) for the olefin to be excited and the H-C-C-H dihedral angel (Θ_{HCCH}) for this olefin. For this grid, the C-C bond length was varied in 0.0025 Å increments and the H-C-C-H dihedral angel was varied in increments of 1°. At each point a relaxed structure was obtained on the singlet energy surface with respect to all other coordinates, then the excitation energy was calculated. Because the E_T for the ω-B97XD/6-31+G** calculations was only 66 kcal/mol, the target excitation energy was 78 kcal/mol (this is 66 + (81-69)). Structure **8** is then the lowest-energy structure found in the grid search that had an excitation energy of 78.0 ± 0.1 kcal/mol.

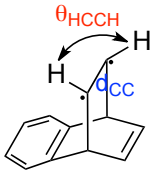

We note that we arrived at the Frutos formalism after alternative model approaches to initiating excited-state trajectories failed because they did not give a proper distribution of zero-point energies in the trajectories. Starting from the formal transition state of the Frutos approach avoids this problem since the zero-point energy + vibrational energy distribution in the starting points is set in a normal thermal statistical way, aside from the excess energy that is present from the difference in geometry between **8** and **2**.

CASSCF+NEVPT2 Calculations

Exploratory CAS calculations were first carried on the model barrelene triplet. This structure exhibited significant interaction between the two singly-occupied orbitals and the π and π* orbitals of each alkene (present as combinations of each), and it was judged that an appropriate active space would include these orbitals, giving six electrons in six active orbitals.

In the optimized structure of triplet barrelene in BP86 calculations these are orbitals 25 through 30 (the counting starts at 0), and they are shown below.

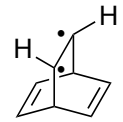

barrelene

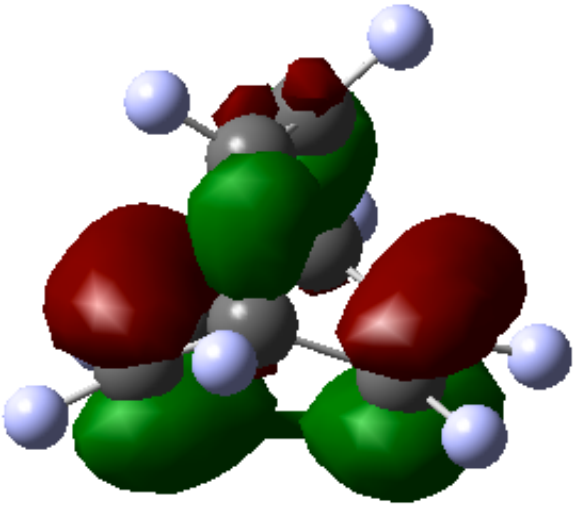

orbital 25

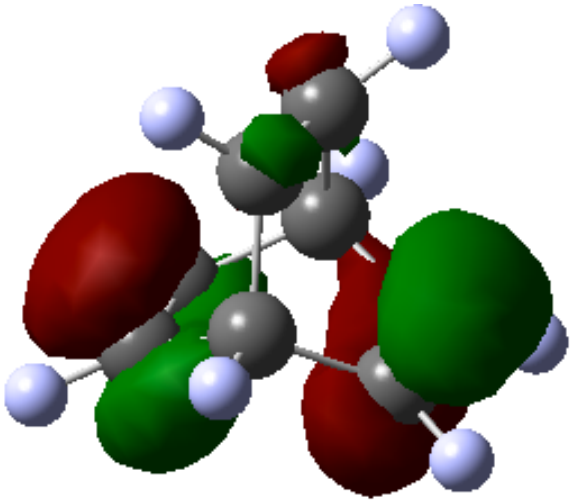

orbital 26

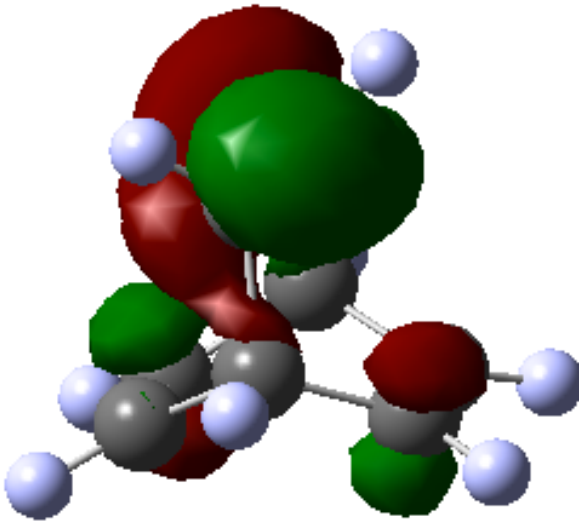

orbital 27

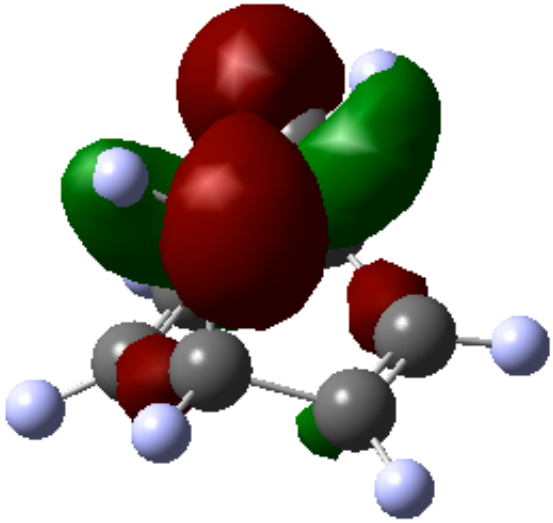

orbital 28

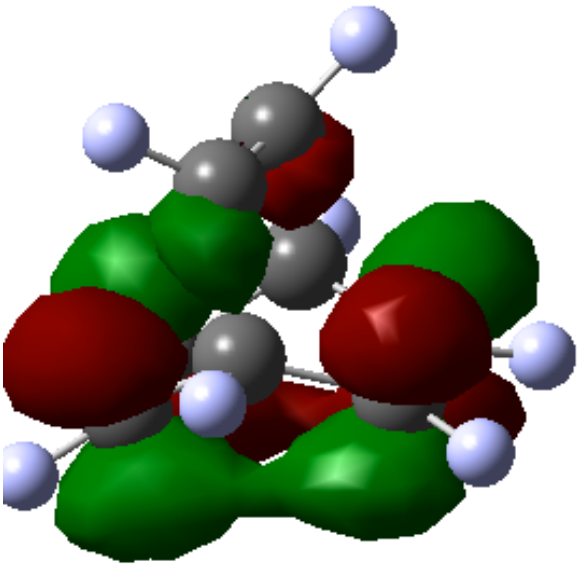

orbital 29

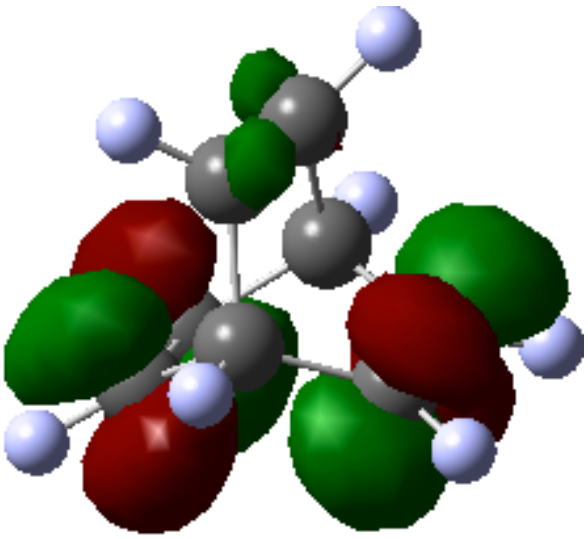

orbital 30

The process for obtaining the right active space consistently for a series of points was to first create and visually examine quasi-restricted orbitals in BP86 calculations employing the desired basis set (ultimately aug-cc-pVTZ, but initially smaller basis sets).

For benzobarrelene, quasi-restricted orbitals were first obtained in BP86 calculations and visualized, leading to a similar set of orbitals were obtained except that the lowest-energy and highest-energy involved aromatic π and π* orbitals. No orbital rotation was required for **anti-2**, and the orbitals for other structures were obtained by calculating them in order as the geometries departed from **anti-2**, in each case reading the previous set of CAS orbitals as a starting point.

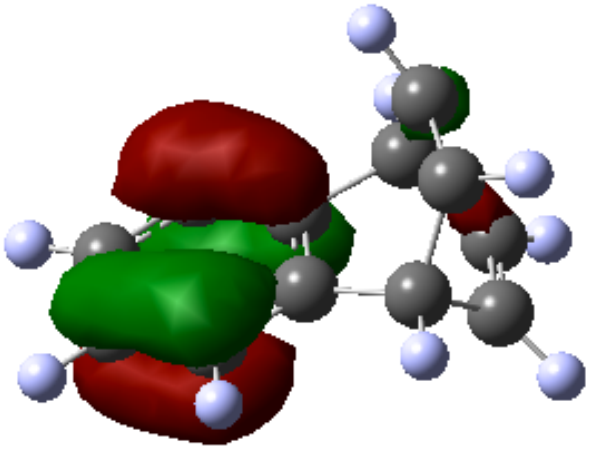

orbital 38

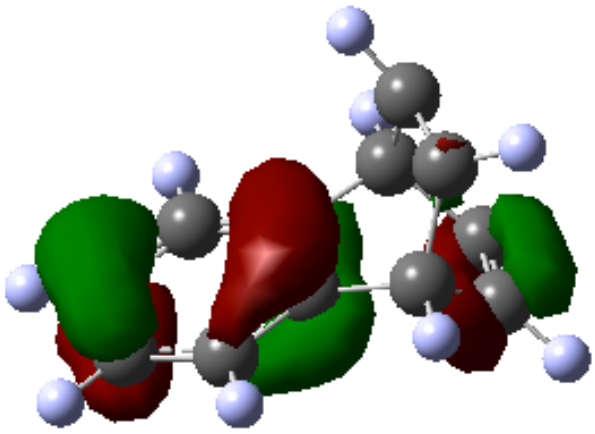

orbital 39

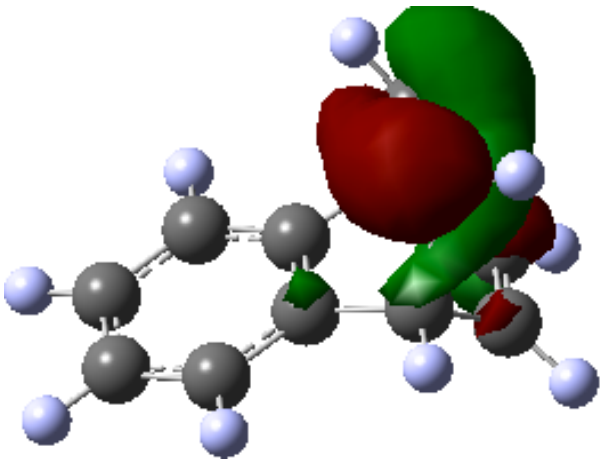

orbital 40

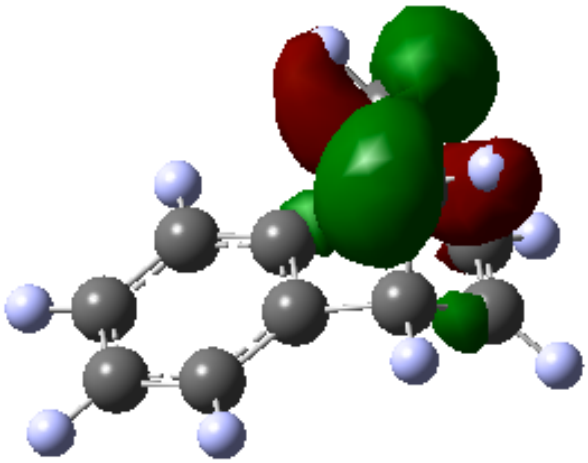

orbital 41

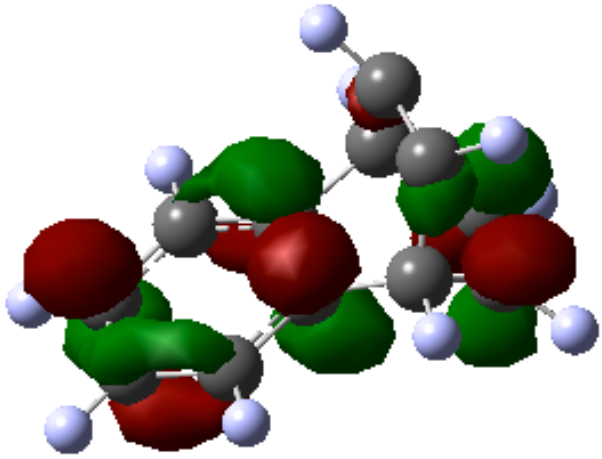

orbital 42

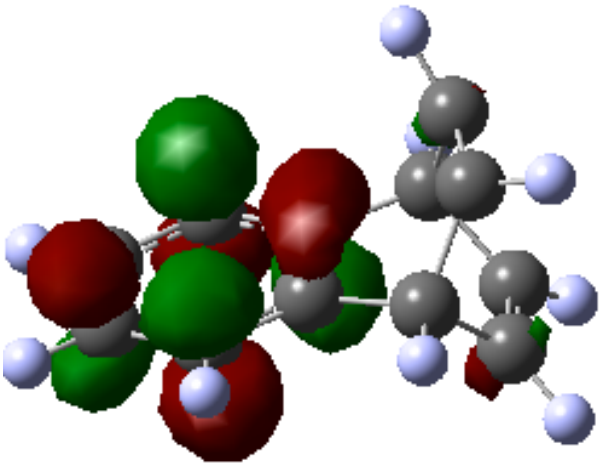

orbital 43

For **anti-2** the final CAS orbital occupancies for orbitals 38 through 43 (starting at 0) were 1.942, 1.9383, 1.00, 1.00, 0.0606, and 0.0591, respectively.

Following the process described above, CASSCF(6,6)+NEVPT2//aug-cc-pVTZ single point energies were calculated for structures along the ω-B97XD/6-31+G** POLYRATE paths for crossing **anti-TS 3**‡, **anti-synTS**, and **synTS 3**‡. The energies obtained are shown in Table S10, along with the reaction coordinate distances *s* in Bohr (based on the original ω-B97XD/6-31+G** paths calculated by POLYRATE) and 0 K energies using the ω-B97XD/6-31+G** zero-point energy corrections. For these paths, the energy given is relative to **anti-2**. The reaction coordinate distance *s* is 0 for the ω-B97XD/6-31+G** saddle points and negative for the reactants.

Table S10. CASSCF(6,6)+NEVPT2//aug-cc-pVTZ energies for POLYRATE path points for reactions of **anti-2** and **syn-2**.

Path from **anti-2** across **anti-TS 3**‡ to **4**			
s (Bohr)	CAS+NEV	0 K	Erel
-2.7	-462.380036	-462.199742	0.00
-2	-462.379240	-462.199151	0.37
-1.5	-462.378113	-462.198259	0.93
-1	-462.376574	-462.197124	1.64
-0.8	-462.375804	-462.196833	1.83
-0.6	-462.375079	-462.196405	2.09
-0.4	-462.374372	-462.195889	2.42
-0.2	-462.374026	-462.195700	**2.54**
-0.1	-462.374064	-462.195809	2.47
0	-462.374352	-462.196167	2.24
0.1	-462.374975	-462.196856	1.81
0.2	-462.376362	-462.198309	0.90
0.4	-462.383071	-462.205129	-3.38
0.6	-462.383545	-462.205680	-3.73
0.8	-462.383659	-462.205813	-3.81
1	-462.384659	-462.206732	-4.39
1.5	-462.388769	-462.210448	-6.72
5	-462.399594	-462.221273	-13.51

Path from **anti-2** across **anti-synTS** to **syn-2**			
s (Bohr)	CAS+NEV	0 K	Erel
-3	-462.380043	-462.199747	0.00
-2	-462.379163	-462.199091	0.41
-1.5	-462.378029	-462.198236	0.95
-1	-462.376650	-462.197640	1.32
-0.8	-462.376145	-462.197244	1.57
-0.6	-462.375674	-462.196836	1.82
-0.4	-462.375263	-462.196473	2.05
-0.2	-462.374915	-462.196140	2.26
-0.1	-462.374767	-462.195984	2.36
0	-462.374627	-462.195817	2.46
0.1	-462.374492	-462.195640	2.57
0.2	-462.374510	-462.195611	2.59
0.4	-462.374395	-462.195431	2.71
0.6	-462.374329	-462.195200	2.85
0.8	-462.374295	-462.195035	2.95
1	-462.374292	-462.194973	2.99
1.5	-462.374325	-462.195002	2.97

2	-462.374296	-462.194967	3.00

Path from **syn-2** across **syn-TS 3**‡ to **4**

s (Bohr)	CAS+NEV	0 K	Erel
-3	-462.374312	-462.194982	2.99
-2	-462.374236	-462.194898	3.04
-1.5	-462.374391	-462.195050	2.94
-1	-462.374332	-462.195322	2.77
-0.8	-462.374330	-462.195429	2.71
-0.6	-462.374310	-462.195472	2.68
-0.4	-462.374325	-462.195535	2.64
-0.2	-462.374473	-462.195698	2.54
-0.1	-462.374592	-462.195809	2.47
0	-462.374803	-462.195993	2.35
0.1	-462.375142	-462.197118	1.65
0.2	-462.375630	-462.197632	1.32
0.4	-462.377940	-462.199954	-0.13
0.6	-462.383121	-462.205031	-3.32
0.8	-462.390298	-462.211988	-7.68
1	-462.388766	-462.210227	-6.58
1.5	-462.388041	-462.209101	-5.87
2	-462.389608	-462.210464	-6.73
3	-462.394826	-462.214662	-9.36
4	-462.397217	-462.218301	-11.65

Programs for Calculations, and Sample Input Files

PROGDYN Usage Details and Configuration Parameters

The trajectories here took as input the output from Gaussian frequency calculations on either structure **2** or structure **8**. For these structures, each normal mode is given a Boltzmann-sampling of thermal excitation and a random phase, and the trajectories are propagated by a Verlet algorithm.

Trajectories started from **2** were carried out using a temperature parameter of 518 K, chosen in order to increase the number of starting trajectories having an energy in the 12 to 14 kcal/mol range as described in the main text. Trajectories were then only considered if they had an energy in the desired range. A total of 525 trajectories were obtained. Of these, 321 (61%) remained in the area of **2**, 183 (35%) cross the **3**‡ to form the intermediate **6**, and 21 (4%) complete the bond-breaking step to afford **6**. The "Statistical" trajectories in Figure 1 in the main text were formed from the 204 trajectories (183 + 21) arranged by the time they crossed the C-C bond-forming distance in **3**‡.

The configuration parameters for trajectories started from **2** (used in program file progdyn.conf) were:

```
method uwB97XD/6-31+g(d,p)
nonstandard 0
rotationmode 1
method2 read
charge 0
multiplicity 3
processors 4
memory 6gb
killcheck 0
checkpoint g16.chk
diagnostics 0
title 3benzobar uwB97XD 2XSM 518dis4
initialdis 4
timestep 1E-15
scaling 1.0
temperature 518
method4 int(finegrid)
methodfile 0
numimag 1
searchdir negative
classical 0
keepevery 9999
highlevel 9999
etolerance 1
damping 1.00
reversetraj false
```

Trajectories started from **8** were carried out using a temperature parameter of 298 K, but otherwise equivalent parameters. A total of 831 trajectories were obtained. Of these, 346 (41.6%) remained in the area of **8**, 438 (52.7%) cross the **3**‡ to form the intermediate **6**, and 47 (5.7%) complete the bond-breaking step to afford **6**. The "Nonstatistical" trajectories in Figure 1 in the main text were formed from the 485 trajectories (438 + 37) arranged by the time they crossed the C-C bond-forming distance in **3**‡.

Example POLYRATE inputs

First Step of the Di-π-methane Rearrangement

```
  TITLE
First step of benzobarrelene dipimethane rearrangement
  END

 ATOMS
  1  C
  2  C
  3  C
  4  C
  5  C
  6  C
  7  C
  8  C
  9  C
  10  C
  11  H
  12  H
  13  H
  14  H
  15  H
  16  H
  17  C
  18  C
  19  H
  20  H
  21  H
  22  H
 END

 NOSUPERMOL
 INPUNIT AU

 WRITEFU31

# MICROCANONICAL RATE CONSTANT

# MDMOVIE ON

*OPTIMIZATION

 OPTMIN  OHOOK
 OPTTS   OHOOK

*SECOND

 HESSCAL HHOOK

 *REACT1
 SPECIES   NONLINRP
 STATUS 2

 *REACT1
 GEOM
1    5.216866455    -1.222955375    -0.109071041
2    2.96228495    -2.59726243    -0.132868071
3    0.67348465    -1.314923624    -0.118198974
4    0.622560713    1.336037939    -0.032369618
5    2.862308291    2.695528013    0.007720947
```

```
6   5.167745939    1.406133402    -0.041016275
7   -1.957283545   -2.490562433   -0.047278441
8   -2.029978309   2.424005287    0.039091647
9   -3.39726049    1.300914767    2.326297394
10  -2.955158404   -1.47702861    2.470869973
11  7.014645254    -2.212488999   -0.145365188
12  2.994861753    -4.651421106   -0.17781323
13  2.821626415    4.74874881     0.076849315
14  6.92693359     2.462824633    -0.022652874
15  -1.888950088   -4.552144282   -0.134258005
16  -2.053022531   4.487569182    -0.002869771
17  -3.537772723   1.233460901    -2.119944843
18  -3.516697668   -1.291309008   -2.141392735
19  -4.538842156   -2.440336948   -3.497091593
20  -4.61610895    2.392896081    -3.424437751
21  -2.06112381    -2.259045791   4.15308375
22  -5.302949202   2.018541065    2.64015773

 END
 ELEC
 3 0.00
 END


 *PROD1
 SPECIES   NONLINRP
 STATUS 2

 *PROD1
 GEOM
1   5.332470089    -1.167987089   -0.000836901
2   3.088282126    -2.554564173   -0.000272272
3   0.779454953    -1.305540177   0.000178305
4   0.69330251     1.35220506     0.00006732
5   2.937703873    2.721975581    -0.000496935
6   5.254641329    1.462125426    -0.000948189
7   -1.818961906   -2.567594344   0.000816448
8   -1.85613721    2.521105165    0.000577053
9   -3.962145451   1.131754777    1.436733335
10  -3.250741081   -1.445921075   2.208913873
11  7.13829826     -2.143226689   -0.001189239
12  3.135379045    -4.609438033   -0.00018298
13  2.878065902    4.776245322    -0.000584292
14  7.000273688    2.541246519    -0.001387379
15  -1.666708136   -4.628601174   0.000882344
16  -1.955245619   4.571902548    0.000496977
17  -3.962785001   1.131613943    -1.434506032
18  -3.251723444   -1.446135897   -2.206752457
19  -2.932929911   -2.015254232   -4.147946745
20  -5.286027702   2.261745026    -2.51574529
21  -2.931080202   -2.014847803   4.150021718
22  -5.284907853   2.26198905     2.518452456

 END
 ELEC
 3 0.00
 END


*START
 SPECIES NONLINTS
 STATUS 2
```

```
 GEOM
1    5.290154555    -1.229159472    -0.054860748
2    3.033451606    -2.59557554    -0.073776712
3    0.74090664    -1.316022404    -0.061457284
4    0.696491703    1.333989576    -0.014284755
5    2.942915361    2.690452168    0.004110622
6    5.245578205    1.401736879    -0.017353849
7    -1.871698444    -2.510575737    -0.030022202
8    -1.904085779    2.476902646    -0.007562702
9    -3.642384331    1.304702832    1.926617107
10    -3.181505264    -1.427590908    2.302381682
11    7.086010308    -2.222845322    -0.069529944
12    3.061512911    -4.650283888    -0.102793714
13    2.903573644    4.744788982    0.035666542
14    7.005464183    2.457247352    -0.003662208
15    -1.780399425    -4.573083126    -0.058875417
16    -1.936203584    4.535176386    -0.084741198
17    -3.656228964    1.204801318    -1.871846217
18    -3.452581893    -1.367451454    -2.121747303
19    -4.653345644    -2.494932672    -3.335319265
20    -5.038263893    2.338349084    -2.877170293
21    -2.777731047    -2.213921813    4.156476136
22    -5.368218748    2.265081501    2.469035275

 END

 ELEC
 3 0.00
 END

# end of start section

*PATH

 SCALEMASS  1.00

 RODS ON

 INTMU   3
 SSTEP   0.01
 INH     10
 NSTEPS  99999
 RPM pagem
 SIGN    PRODUCT


 SRANGE
  SLP   4.00
  SLM  -4.00
 END

 COORD  CART

 PRPATH
  COORD 9 25
  INTERVAL 1
  XMOL
 END

 PRSAVERP

 #SPECSTOP
```

```
 #PERCENTDOWN 99.
 #END

*TUNNEL

QUAD
 NQE   40
 NQTH  40
END

 ZCT
 SCT

 *RATE
   GTLOG
   BOTHK
   SIGMAF 1
   TST
   CVT

  TEMP
   77
   100
   120
   200
   300
   400
   487
   500
   568
```

Second Step of the Di-π-methane Rearrangement

```
  TITLE
Second step of benzobarrelene dipimethane rearrangement
  END

 ATOMS
   1  C
   2  C
   3  C
   4  C
   5  C
   6  C
   7  C
   8  C
   9  C
  10  C
  11  H
  12  H
  13  H
  14  H
  15  H
  16  H
  17  C
  18  C
  19  H
  20  H
  21  H
  22  H
 END
```

```
 NOSUPERMOL
 INPUNIT AU

 WRITEFU31

# MICROCANONICAL RATE CONSTANT

# MDMOVIE ON

*OPTIMIZATION

 OPTMIN  OHOOK
 OPTTS   OHOOK

 *SECOND

 HESSCAL HHOOK

 *REACT1
 SPECIES   NONLINRP
 STATUS 2

 *REACT1
 GEOM
1    5.332470089    -1.167987089    -0.000836901
2    3.088282126    -2.554564173    -0.000272272
3    0.779454953    -1.305540177     0.000178305
4    0.69330251     1.35220506      0.00006732
5    2.937703873     2.721975581    -0.000496935
6    5.254641329     1.462125426    -0.000948189
7    -1.818961906    -2.567594344     0.000816448
8    -1.85613721     2.521105165     0.000577053
9    -3.962145451     1.131754777     1.436733335
10    -3.250741081    -1.445921075     2.208913873
11    7.13829826     -2.143226689    -0.001189239
12    3.135379045     -4.609438033    -0.00018298
13    2.878065902     4.776245322    -0.000584292
14    7.000273688     2.541246519    -0.001387379
15    -1.666708136    -4.628601174     0.000882344
16    -1.955245619     4.571902548     0.000496977
17    -3.962785001     1.131613943    -1.434506032
18    -3.251723444    -1.446135897    -2.206752457
19    -2.932929911    -2.015254232    -4.147946745
20    -5.286027702     2.261745026    -2.51574529
21    -2.931080202    -2.014847803     4.150021718
22    -5.284907853     2.26198905     2.518452456

 END
 ELEC
 3 0.00
 END


 *PROD1
 SPECIES   NONLINRP
 STATUS 2

 *PROD1
 GEOM
1    -5.316685696    -1.246824174     0.222035821
2    -3.002661274    -2.510790157     0.084413403
```

```
3    -0.756312387    -1.18534335    -0.160050411
4    -0.795699142    1.516941344    -0.311607047
5    -3.15940324    2.752441587    -0.14054668
6    -5.380360797    1.391699321    0.115518261
7    1.828364361    -2.474921033    -0.245425324
8    1.496642239    2.876221621    -0.643370275
9    3.952975102    1.405600676    -0.798955615
10    3.371444985    -1.033893426    -2.159040588
11    -7.057888701    -2.314135992    0.418470673
12    -2.948066062    -4.563543135    0.181817593
13    -3.208766779    4.804683011    -0.23711147
14    -7.175908387    2.379245447    0.228381136
15    1.629930265    -4.503067951    -0.596763241
16    1.487302081    4.928141115    -0.645208481
17    4.455871667    0.388442537    1.872318659
18    3.238637459    -1.796147659    2.182367977
19    3.058266467    -2.863219336    3.923048986
20    5.456089649    1.454083859    3.309415984
21    2.960953513    -1.092067532    -4.168662891
22    5.483781292    2.534570432    -1.604422655

 END
 ELEC
 3 0.00
 END


 *START
 SPECIES NONLINTS
 STATUS 2
 GEOM
1    5.321282028    -1.235620455    -0.05792103
2    3.046453754    -2.564165338    0.085798377
3    0.764194835    -1.274489995    0.166366506
4    0.728509584    1.40155421    0.132139472
5    3.020874185    2.709023583    -0.069408831
6    5.29875031    1.398270402    -0.147818134
7    -1.84036997    -2.528205316    0.181179512
8    -1.702804043    2.661452788    0.243050298
9    -3.996782129    1.279945892    1.180426323
10    -3.330039265    -1.237738909    2.250647002
11    7.101716368    -2.254023665    -0.117242388
12    3.04824737    -4.619775696    0.114853871
13    3.007487587    4.763284662    -0.128269187
14    7.06484198    2.435609993    -0.277969464
15    -1.68554191    -4.583568825    0.340097362
16    -1.831940958    4.675841687    -0.126823291
17    -4.185783514    0.78591035    -1.624951642
18    -3.19272272    -1.56798817    -2.16360133
19    -2.903645894    -2.352396986    -4.031960057
20    -5.126560142    2.049892981    -2.92832789
21    -2.936712149    -1.538278083    4.239378865
22    -5.44225304    2.414481904    2.104614634
 END

 ELEC
 3 0.00
 END

# end of start section

*PATH
```

```
 SCALEMASS  1.00

 RODS ON

 INTMU   3
 SSTEP   0.01
 INH     10
 NSTEPS  99999
 RPM pagem
 SIGN    PRODUCT


 SRANGE
  SLP   2.60
  SLM  -2.20
 END

 COORD  CART

 PRPATH
  COORD 9 25
  INTERVAL 1
  XMOL
 END

 PRSAVERP

 #SPECSTOP
 #PERCENTDOWN 99.
 #END

*TUNNEL

QUAD
 NQE   40
 NQTH  40
END

 ZCT
 SCT

 *RATE
   GTLOG
   BOTHK
   SIGMAF 1
   TST
   CVT

  TEMP
   77
   100
   120
   200
   300
   400
   487
   500
   568
```

RRKM Calculations

RRKM calculations were based on the frequencies in optimized structures for **2**, **3**‡, **4**, and **5**‡ including ^{13}C in the relevant positions. An example input file is given below. The threshold energy barriers in each calculation were the differences between the zero-point level energies for the **3**‡ versus **2** or **5**‡ versus **4**. The nominal KIE was then calculated using eqs S1 through S6.

Tunneling corrections for the RRKM rate constants were estimated using the equation below for the transmission coefficient (G), where V_0 is the classical E+zpe barrier, E is the microcanonical energy, and ν* is the imaginary frequency of the transition state. It was found that the tunneling correction was negligible in the high-energy realm of interest, and the reported nominal KIE in the main text is not tunneling corrected.

$$G = \frac{1}{1 + \exp\left[\frac{2\pi(V_0 - E)}{h\nu^*}\right]}$$

Sample RRKM Input for Unlabeled Isotopomer

```
0,0.1,301
0
-1,0,1,10
0
0
0
1.0
60,0
124.4239,170.2000,276.0117,318.3819,354.9149,377.6504,430.3171
505.0296,513.3253,534.4443,579.4522,631.5954,653.8064,655.8322
722.5026,772.1473,777.7874,798.5469,811.0521,833.2601,898.4797
901.3637,931.9622,959.7746,966.7662,969.6294,976.2146,1001.0930
1009.4800,1064.2046,1101.0508,1132.5956,1138.2221,1185.7406,1190.4919
1191.4661,1221.6087,1227.9069,1246.5392,1268.5326,1302.3970,1328.9446
1354.7775,1376.2255,1382.9124,1509.4858,1524.5552,1661.8962,1678.1694
1687.4079,3134.8019,3137.0392,3152.6303,3164.7169,3199.0546,3203.5555
3216.7188,3221.6750,3231.3673,3246.5708
404.05,404.05,643.28
0
2.918
59,0
124.9097,166.6127,194.8289,345.5069,377.4768,420.2073,455.2271
469.3747,521.0664,534.9264,556.7006,591.9112,653.4248,667.3212
682.1649,776.8157,784.4243,789.9482,814.8841,865.0691,899.4059
910.7498,947.2153,963.2776,969.3937,975.2466,1009.8379,1014.9739
1066.1782,1084.7793,1123.3590,1142.1735,1166.5325,1191.3429,1197.5879
1227.3338,1238.7689,1264.1512,1269.8335,1301.7233,1337.4495,1358.1468
1371.3809,1392.1804,1496.7868,1512.2880,1537.9647,1668.2771,1691.5781
3138.0274,3158.4226,3197.6031,3201.6456,3216.0041,3219.4989,3230.6306
3231.0659,3240.3116,3258.3600
402.44,402.44,665.75
0
```

Calculated Structures and Complete Energies

Guide to Structures and Structure Titles

Table S11 lists the structures of importance this study and some relevant raw energies. All of the structures were obtained on a ω-B97XD/6-31+G** surface, and the wb97xd suffix indicates the energies given are for this surface. The DLPNO suffix represents the DLPNO-CCSD(T) single-point energies at the DFT optimized structures. The tripletgeom or singletgeom suffix indicate the single-point energies of singlet/triplet state at triplet/singlet optimized geometry. The CAS suffix indicated single-point energies obtained in CASSCF(6,6)+NEVPT2//aug-cc-pVTZ calculations. The CAS energies are for the points given but it should be noted that the position of the transition states changes somewhat between the CASSCF(6,6)+NEVPT2//aug-cc-pVTZ and ω-B97XD/6-31+G** calculations.

Table S11. List of structures optimized by Uω-B97XD/6-31+G** level of theory.

File name	Pot E.	E+zpe	H	S (e.u.)	G
ωB97XD/6-31+g(d,p) structures					
acetone-singlet-wb97xd	-193.10795	-193.02363	-193.017326	72.505	-193.051776
acetone-singlet-DLPNO	-192.849752				
acetone-triplet-wb97xd	-192.984531	-192.902408	-192.896102	73.202	-192.930882
acetone-triplet-DLPNO	-192.720712				
acetone-singlet-tripletgeom	-193.06571				
acetone-triplet-singletgeom	-192.962479				
acetophenone-singlet-wb97xd	-384.788408	-384.649083	-384.640386	87.175	-384.681806
acetophenone-singlet-DLPNO	-384.231542				
acetophenone-triplet-wb97xd	-384.674386	-384.538813	-384.529451	92.509	-384.573441
acetophenone-triplet-DLPNO	-384.114983				
acetophenone-singlet-tripletgeom	-384.770216				
acetophenone-triplet-singletgeom	-384.660149				
1	-463.116772	-462.933273	-462.924453	86.945	-462.965764
1-DLPNO	-462.400891				
2	-463.013235	-462.832944	-462.823675	90.837	-462.866853
2-DLPNO	-462.290656				
1-triplet-SinglePoint	-462.968147				
2-singlet-SinglePoint	-463.037849				
syn-2	-463.009071	-462.829734	-462.819968	93.218	-462.864258
syn-2-DLPNO	-462.286739				
anti-TS 3‡	-463.006917	-462.82873	-462.819447	91.098	-462.862730
anti-TS 3‡-DLPNO	-462.283947				
anti-TS 3‡-CAS	-462.374352				
syn-TS 3‡-syn	-463.008191	-462.830127	-462.820772	91.234	-462.864120
syn-TS 3‡-DLPNO	-462.286627				
syn-TS 3‡-CAS	-462.374803				
anti-synTS	-463.008785	-462.829973	-462.820773	90.711	-462.863873
anti-synTS-DLPNO	-462.285960				

4	-463.033276	-462.853198	-462.844043	90.349	-462.886970
4-DLPNO	-462.305251				
5‡	-463.020231	-462.841426	-462.8325	89.608	-462.875075
5‡-DLPNO	-462.295433				
6	-463.037848	-462.857972	-462.848616	91.323	-462.892007
6-DLPNO	-462.315353				
7	-463.114941	-462.931177	-462.922495	86.804	-462.963738
7-DLPNO	-462.393032				

acetone-singlet

/home/hanyclose/dipimethane/paper/acetone-singlet-wb97xd
opt
E(UwB97XD) = -193.107950179

Zero-point correction= 0.084320 (Hartree/Particle)
Thermal correction to Energy= 0.089680
Thermal correction to Enthalpy= 0.090624
Thermal correction to Gibbs Free Energy= 0.056175
Sum of electronic and ZPE= -193.023630
Sum of electronic and thermal Energies= -193.018270
Sum of electronic and thermal Enthalpies= -193.017326
Sum of electronic and thermal Free Energies= -193.051776

	E	CV	S
	KCal/Mol	Cal/Mol-K	Cal/Mol-K
Total	56.275	16.730	72.505

C,0,-1.6466485106,0.1463433668,-0.0212561374
C,0,-0.1592597346,0.1071567622,0.2567602367
H,0,-1.9343258194,-0.6594979678,-0.7044008478
H,0,-1.9242850166,1.1128749894,-0.4425175117
H,0,-2.1957960229,-0.0134959578,0.9135484721
C,0,0.4157731123,-1.2297037578,0.6732386337
O,0,0.5364118429,1.0964748384,0.1510548959
H,0,0.3640414358,-1.9267192965,-0.1708540987
H,0,-0.1711473933,-1.6672892259,1.4873874734
H,0,1.4551257624,-1.1116387349,0.9808372638

acetone-triplet

/home/hanyclose/dipimethane/paper/acetone-triplet-wb97xd
opt
E(UwB97XD) = -192.984531382

Zero-point correction= 0.082124 (Hartree/Particle)
Thermal correction to Energy= 0.087485
Thermal correction to Enthalpy= 0.088430
Thermal correction to Gibbs Free Energy= 0.053649
Sum of electronic and ZPE= -192.902408
Sum of electronic and thermal Energies= -192.897046
Sum of electronic and thermal Enthalpies= -192.896102
Sum of electronic and thermal Free Energies= -192.930882

	E	CV	S
	KCal/Mol	Cal/Mol-K	Cal/Mol-K
Total	54.898	17.428	73.202

C,0,-7.4327403373,0.7221137913,-0.018503117
C,0,-6.0345308071,0.3423962121,-0.4643988416
H,0,-8.0506557714,-0.1793162904,-0.0073847933
H,0,-7.8811544461,1.4445414347,-0.7040231885
H,0,-7.425618286,1.1592944845,0.9916133499
C,0,-5.3171565236,-0.7572990185,0.2932573236
H,0,-5.1117977804,-0.458743843,1.3325867
H,0,-4.3693902464,-1.011210452,-0.1865163202
H,0,-5.9537208501,-1.6456880615,0.3016274758
O,0,-5.2660049692,1.3905717293,-0.7055985778

acetophenone-singlet

/home/hanyclose/dipimethane/paper/acetophenone-singlet-wb97xd
uwB97XD/6-31+g(d,p)
E(UwB97XD) = -384.788408366

Zero-point correction= 0.139325 (Hartree/Particle)
Thermal correction to Energy= 0.147078
Thermal correction to Enthalpy= 0.148023
Thermal correction to Gibbs Free Energy= 0.106603
Sum of electronic and ZPE= -384.649083
Sum of electronic and thermal Energies= -384.641330
Sum of electronic and thermal Enthalpies= -384.640386
Sum of electronic and thermal Free Energies= -384.681806

	E	CV	S
	KCal/Mol	Cal/Mol-K	Cal/Mol-K
Total	92.293	29.320	87.175

C,0,-2.1025175891,1.370512314,-0.6178558442
C,0,-0.8519649828,1.5916000324,-0.0299896912
C,0,-0.053841012,0.4953530536,0.3133773387
C,0,-0.4993609689,-0.8018326867,0.0726164018
C,0,-1.745543196,-1.0122802304,-0.5129265635
C,0,-2.5470565384,0.076300866,-0.8580697647
H,0,-2.7099255146,2.2308900199,-0.8785053243
C,0,-0.4169464221,3.0080767151,0.2089077718
H,0,-2.0925527045,-2.0237240563,-0.7004723806
H,0,-3.51821636,-0.0868107064,-1.3143794711
H,0,0.9193274673,0.6435586715,0.7702004166
H,0,0.1260215477,-1.6469381587,0.3420166052
O,0,-1.1388311262,3.9376702716,-0.1036581977

C,0,0.9332741563,3.259985235,0.8442999339
H,0,1.7353287704,2.8359604522,0.2314492068
H,0,0.9896562451,2.7938935753,1.8333439822
H,0,1.0799682276,4.3355346317,0.9407755804

acetophenone-triplet

/home/hanyclose/dipimethane/paper/acetophenone-triplet-wb97xd
opt
E(UwB97XD) = -384.674385854

Zero-point correction= 0.135572 (Hartree/Particle)
Thermal correction to Energy= 0.143991
Thermal correction to Enthalpy= 0.144935
Thermal correction to Gibbs Free Energy= 0.100981
Sum of electronic and ZPE= -384.538813
Sum of electronic and thermal Energies= -384.530395
Sum of electronic and thermal Enthalpies= -384.529451
Sum of electronic and thermal Free Energies= -384.573405

	E	CV	S
	KCal/Mol	Cal/Mol-K	Cal/Mol-K
Total	90.356	30.997	92.509

C,0,-2.0174658711,1.229026802,-0.0724787523
C,0,-0.6066809819,1.4062108819,-0.0542482799
C,0,-2.5697948984,-0.0240147934,0.1296141684
C,0,0.2083375316,0.2658980746,0.17588627
C,0,-0.3667811933,-0.9786531928,0.3756986752
C,0,-1.7556986344,-1.1392445376,0.3553334013
H,0,-3.6495773078,-0.1379117676,0.1118329253
H,0,-2.1967758966,-2.1177418562,0.5128134059
H,0,1.2889605758,0.3653985515,0.1961448036
H,0,0.274404442,-1.8375809041,0.550005253
H,0,-2.6619389112,2.0853419949,-0.2464201508
C,0,-0.0253241545,2.6808740619,-0.2590701745
O,0,-0.7688008189,3.7512952508,-0.4749481054
C,0,1.4513655948,2.9943623717,-0.2625154856
H,0,1.8959296607,2.7347352557,0.704498912
H,0,1.6193272226,4.0577185676,-0.4432758819
H,0,1.9574136406,2.4266052394,-1.0510309843

1

/home/hanyclose/dipimethane/paper/benzobarrelene-singlet
opt
E(UwB97XD) = -463.116771824

Zero-point correction= 0.183499 (Hartree/Particle)
Thermal correction to Energy= 0.191374
Thermal correction to Enthalpy= 0.192319
Thermal correction to Gibbs Free Energy= 0.151008
Sum of electronic and ZPE= -462.933273
Sum of electronic and thermal Energies= -462.925397
Sum of electronic and thermal Enthalpies= -462.924453
Sum of electronic and thermal Free Energies= -462.965764

	E	CV	S
	KCal/Mol	Cal/Mol-K	Cal/Mol-K
Total	120.089	34.976	86.945

C,0,2.7659340629,-0.595268077,-0.0967894781
C,0,1.5822573984,-1.3461789051,-0.0596057925
C,0,0.3672194617,-0.6868057294,-0.0220152935
C,0,0.3169547059,0.7122837272,-0.0210190193
C,0,1.481537381,1.4572071219,-0.0576047219
C,0,2.7160488929,0.7932314651,-0.0957970981
C,0,-1.0275811456,-1.3150971855,0.0216696095
C,0,-1.1193344999,1.2388042642,0.0235568651
C,0,-1.7377609498,0.6029543123,1.2726866975
C,0,-1.6900222132,-0.7271065319,1.271680411
H,0,3.724885884,-1.1033107756,-0.1264642843
H,0,1.6211124439,-2.432181965,-0.0603870713
H,0,1.4423523887,2.5431980886,-0.0568151899
H,0,3.6360694809,1.3688212691,-0.1246914772
H,0,-0.9964425842,-2.4051213104,0.0211215777
H,0,-1.1664933634,2.3282524319,0.0246191551
C,0,-1.8143796611,0.6020170464,-1.1841097122
C,0,-1.7665467105,-0.7280442555,-1.1851225741
H,0,-2.1785040095,-1.3688445686,-1.955683237
H,0,-2.2713315208,1.2127348231,-1.9537309483
H,0,-2.0531899036,-1.3673292067,2.0668667054
H,0,-2.1458625388,1.214292961,2.0688118764

2

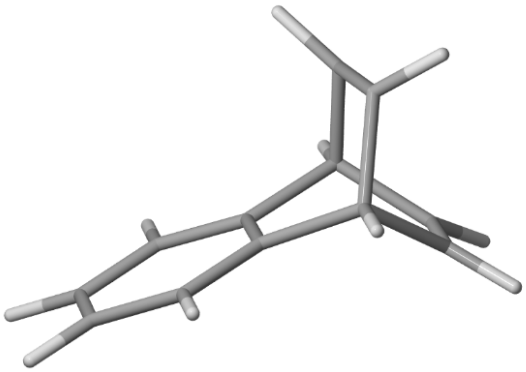

/home/hanyclose/dipimethane/paper/benzobarrelene-triplet
opt
E(UwB97XD) = -463.013234922

Zero-point correction= 0.180291 (Hartree/Particle)
Thermal correction to Energy= 0.188616
Thermal correction to Enthalpy= 0.189560
Thermal correction to Gibbs Free Energy= 0.146400
Sum of electronic and ZPE= -462.832944
Sum of electronic and thermal Energies= -462.824619
Sum of electronic and thermal Enthalpies= -462.823675
Sum of electronic and thermal Free Energies= -462.866835

	E	CV	S
	KCal/Mol	Cal/Mol-K	Cal/Mol-K
Total	118.358	36.377	90.837

C,0,2.7640434681,-0.6462665805,-0.0575187887
C,0,1.5713378298,-1.373830889,-0.0683736103
C,0,0.3592740832,-0.69531679,-0.0613294476
C,0,0.3316715883,0.7072137096,-0.0190975966
C,0,1.5166919914,1.427510018,-0.0000984318
C,0,2.7370801757,0.7458197678,-0.0243438888
C,0,-1.0309090443,-1.319237428,-0.0280302267
C,0,-1.0704860114,1.2834014825,0.017831171
C,0,-1.8020962712,0.6863330577,1.2195201716
C,0,-1.5618464606,-0.7817135887,1.3006625059
H,0,3.7153106361,-1.1691463307,-0.0757824047
H,0,1.5902326683,-2.4602004298,-0.089824632
H,0,1.4959575999,2.5134121637,0.0351216616
H,0,3.6674008786,1.3051951683,-0.0154588368
H,0,-0.9956398109,-2.4093088862,-0.0735572156
H,0,-1.0855130438,2.3743924073,-0.0036267011
C,0,-1.8727123862,0.6531501022,-1.1192697153
C,0,-1.8567848926,-0.6856433944,-1.1347536547

H,0,-2.401779554,-1.291916859,-1.849492838
H,0,-2.4539251622,1.2650168467,-1.8012332296
H,0,-1.1322274491,-1.2136097904,2.2038423903
H,0,-2.7981588332,1.0832562429,1.4159913179

syn-2

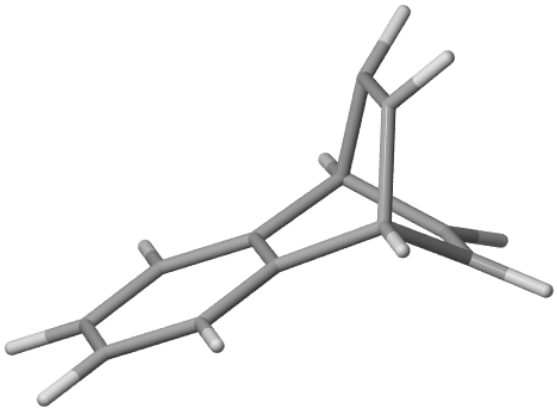

/home/hanyclose/dipimethane/benzobarrelene-triplet-syn
opt
E(UwB97XD) = -463.009071055

Zero-point correction= 0.179337 (Hartree/Particle)
Thermal correction to Energy= 0.188159
Thermal correction to Enthalpy= 0.189104
Thermal correction to Gibbs Free Energy= 0.144813
Sum of electronic and ZPE= -462.829734
Sum of electronic and thermal Energies= -462.820912
Sum of electronic and thermal Enthalpies= -462.819968
Sum of electronic and thermal Free Energies= -462.864258

	E	CV	S
	KCal/Mol	Cal/Mol-K	Cal/Mol-K
Total	118.072	37.399	93.218

C,0,2.7600284795,-0.7199041182,0.0110331894
C,0,1.5465313877,-1.4107239122,0.0053587445
C,0,0.3546069124,-0.6982961193,-0.0196633589
C,0,0.3693476541,0.701788289,-0.0328157299
C,0,1.5760188324,1.3892955843,-0.020948706
C,0,2.7746996388,0.6733001819,-0.0020309376
C,0,-1.0371042581,-1.2899704962,-0.0177687705
C,0,-1.0095788636,1.3225986322,-0.0423220695
C,0,-1.7778530455,0.7939892114,1.1575022714
C,0,-1.7937283062,-0.7228261916,1.171819144
H,0,3.6951554096,-1.2711879242,0.0261991503
H,0,1.5334457602,-2.4972997209,0.0197227487
H,0,1.5858305206,2.4759840725,-0.0270086194
H,0,3.7212305328,1.2049589647,0.0029647247
H,0,-1.0370001263,-2.3801595132,-0.0435515741
H,0,-0.9864785374,2.4118675724,-0.0885833391
C,0,-1.8458065986,0.6908159725,-1.1399789328
C,0,-1.8600485832,-0.6614352,-1.1272769093
H,0,-2.5004268701,-1.2649113364,-1.7615946472
H,0,-2.4734702769,1.2955970477,-1.7856616577
H,0,-2.6663652805,-1.2561157454,1.5398810375
H,0,-2.6392573819,1.3522307492,1.5149102415

anti-TS 3‡

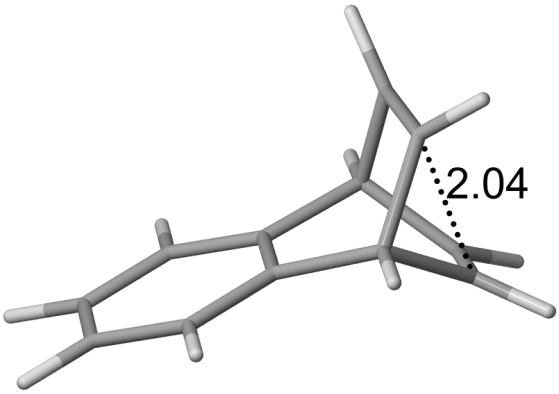

/home/hanyclose/dipimethane/paper/DPM-TS1
opt=(ts,calcfc,noeigentest)
E(UwB97XD) = -463.006916991

Zero-point correction= 0.178187 (Hartree/Particle)
Thermal correction to Energy= 0.186526
Thermal correction to Enthalpy= 0.187470
Thermal correction to Gibbs Free Energy= 0.144187
Sum of electronic and ZPE= -462.828730
Sum of electronic and thermal Energies= -462.820391
Sum of electronic and thermal Enthalpies= -462.819447
Sum of electronic and thermal Free Energies= -462.862730

	E	CV	S
	KCal/Mol	Cal/Mol-K	Cal/Mol-K
Total	117.047	36.013	91.098

C,0,2.8063312875,-0.6439499163,-0.0310048655
C,0,1.6132437977,-1.3692014389,-0.0356276516
C,0,0.3991548887,-0.6930415654,-0.0317778531
C,0,0.3730150637,0.7085022795,-0.0146966875
C,0,1.5603240934,1.4289663487,-0.0093713625
C,0,2.7801936017,0.7488619864,-0.0183198433
C,0,-0.9809206642,-1.327291917,-0.0121188228
C,0,-1.0062006051,1.3075490724,-0.0095339753
C,0,-1.9094660273,0.6942256764,1.0346926305
C,0,-1.6863428986,-0.7578996031,1.2095808845
H,0,3.7572040403,-1.1679031831,-0.0375380695
H,0,1.6312838439,-2.4558666536,-0.0451531932
H,0,1.5393895928,2.5155116594,0.0024763005
H,0,3.710320378,1.3085998599,-0.0149328165
H,0,-0.935202462,-2.417696166,-0.0262106837
H,0,-1.0247688689,2.3960316342,-0.047046974
C,0,-1.926252548,0.6400016075,-1.0017196741
C,0,-1.8257301578,-0.7266731006,-1.1166749194
H,0,-2.4704950685,-1.3274180568,-1.7455704637
H,0,-2.6578246811,1.2342111363,-1.5386922603
H,0,-1.612995746,-1.2333931779,2.1825073499
H,0,-2.7989958601,1.2181685182,1.3645439503

syn-TS 3‡

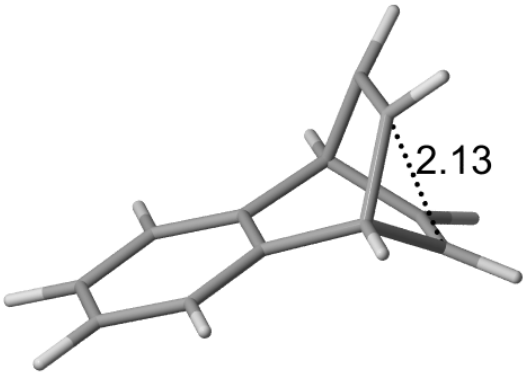

/home/hanyclose/dipimethane/synTS1.log
opt=(ts,calcfc,noeigentest)
Zero-point correction= 0.178063 (Hartree/Particle)
Thermal correction to Energy= 0.186475
Thermal correction to Enthalpy= 0.187419
Thermal correction to Gibbs Free Energy= 0.144071
Sum of electronic and ZPE= -462.830128
Sum of electronic and thermal Energies= -462.821716
Sum of electronic and thermal Enthalpies= -462.820772
Sum of electronic and thermal Free Energies= -462.864120

	E	CV	S
	KCal/Mol	Cal/Mol-K	Cal/Mol-K
Total	117.015	36.346	91.234

C,0,2.7811379457,-0.6584379951,0.0011035488
C,0,1.577626574,-1.3655557556,-0.0167694196
C,0,0.3746137786,-0.6707450221,-0.0314948151
C,0,0.3697134193,0.7288476766,-0.0266395995
C,0,1.5672048106,1.4330057292,-0.0074104142
C,0,2.776087291,0.7349527525,0.0059502845
C,0,-1.0028952031,-1.2886673588,-0.0456208031
C,0,-1.0068030468,1.3395882393,-0.045315562
C,0,-1.8892668955,0.7571840846,1.0314352848
C,0,-1.8286967082,-0.7183330392,1.0927263403
H,0,3.7238487882,-1.1967816048,0.0116423496
H,0,1.5798341481,-2.4523343843,-0.0189039524
H,0,1.5614788446,2.5197913154,-0.0028177184
H,0,3.714684059,1.2802954842,0.0201298692
H,0,-0.9837437062,-2.3781366871,-0.0651484426
H,0,-1.0045438648,2.4285127454,-0.0717748247
C,0,-1.8854553683,0.7059394146,-1.0963010345
C,0,-1.8490773166,-0.673202657,-1.1386302767
H,0,-2.5363170832,-1.2715353256,-1.7253735842
H,0,-2.5913088956,1.3052029863,-1.6600674991
H,0,-2.6290395659,-1.3011486832,1.535902333
H,0,-2.7216643249,1.3251062948,1.4298649256

anti-synTS

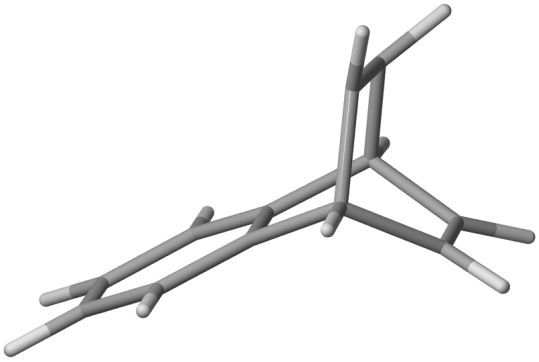

/home/hanyclose/dipimethane/benzo-wb97xd-TStt-2
opt=(ts,calcfc,noeigentest)
E(UwB97XD) = -463.008784974

Zero-point correction= 0.178812 (Hartree/Particle)
Thermal correction to Energy= 0.187068
Thermal correction to Enthalpy= 0.188012
Thermal correction to Gibbs Free Energy= 0.144912
Sum of electronic and ZPE= -462.829973
Sum of electronic and thermal Energies= -462.821717
Sum of electronic and thermal Enthalpies= -462.820773
Sum of electronic and thermal Free Energies= -462.863873

	E	CV	S
	KCal/Mol	Cal/Mol-K	Cal/Mol-K
Total	117.387	35.684	90.711

C,0,2.7400505967,-0.7224207235,-0.0561019285
C,0,1.5239859468,-1.4093466186,-0.0297654326
C,0,0.3343567624,-0.6936891636,-0.0303614723
C,0,0.3545770968,0.7072883866,-0.053180086
C,0,1.5632367564,1.3910479007,-0.070895268
C,0,2.7595503418,0.670418383,-0.0767377176
C,0,-1.058159365,-1.2836774473,-0.0029766793
C,0,-1.0297168427,1.3267469255,-0.0141700883
C,0,-1.6838196867,0.7810859312,1.2415605798
C,0,-1.8140615767,-0.7250828409,1.1932446067
H,0,3.6732578314,-1.2771041333,-0.0601142797
H,0,1.5081789928,-2.4957743714,-0.0091749619
H,0,1.5764146555,2.477672654,-0.0821505266
H,0,3.7079472305,1.1984435855,-0.0969816583
H,0,-1.0617409315,-2.3737154262,-0.0418242844
H,0,-1.0053104725,2.4165675777,-0.0481938389
C,0,-1.8850235338,0.7040247098,-1.1044375741
C,0,-1.8979103167,-0.6443675174,-1.0976889054
H,0,-2.5423529074,-1.2465709597,-1.7295395899
H,0,-2.5079526278,1.3128610501,-1.7506261221
H,0,-2.7768789005,-1.1848273232,1.4182071046
H,0,-2.2382944795,1.4019358811,1.9336904126

4

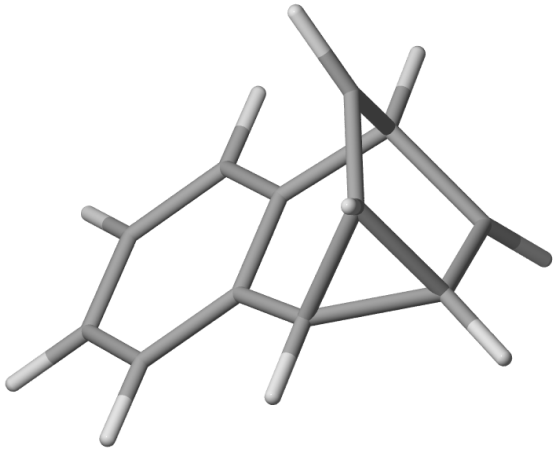

/home/hanyclose/dipimethane/paper/DPM-IM
opt
E(UwB97XD) = -463.033276343

Zero-point correction= 0.180078 (Hartree/Particle)
Thermal correction to Energy= 0.188289
Thermal correction to Enthalpy= 0.189234
Thermal correction to Gibbs Free Energy= 0.146306
Sum of electronic and ZPE= -462.853198
Sum of electronic and thermal Energies= -462.844987
Sum of electronic and thermal Enthalpies= -462.844043
Sum of electronic and thermal Free Energies= -462.886970

	E	CV	S
	KCal/Mol	Cal/Mol-K	Cal/Mol-K
Total	118.153	36.255	90.349

C,0,2.8268853688,-0.6155563176,-0.0004450348
C,0,1.6388018858,-1.3491086147,-0.00014544
C,0,0.4173929804,-0.6869659441,0.000093485
C,0,0.3718920301,0.7190344252,0.0000350479
C,0,1.5596381493,1.4437282974,-0.0002640109
C,0,2.7860352325,0.7765311962,-0.0005038166
C,0,-0.9585930802,-1.3557690641,0.0004316593
C,0,-0.9774698023,1.3377312897,0.0003044725
C,0,-2.0939880827,0.5998314265,0.7639369995
C,0,-1.7130349967,-0.760459662,1.1686677534
H,0,3.781944346,-1.1317645443,-0.0006319482
H,0,1.6649829912,-2.435788169,-0.0000982586
H,0,1.5305919621,2.5302570506,-0.0003105372
H,0,3.7096895359,1.3469429321,-0.0007367561
H,0,-0.8799737664,-2.4454235374,0.0004673701
H,0,-1.0310603837,2.4225175926,0.0002635272
C,0,-2.094327045,0.5997569829,-0.7627602092
C,0,-1.7135537695,-0.7605736393,-1.1675273461
H,0,-1.5980273976,-1.091935437,-2.1927578958
H,0,-2.7949257946,1.1951063614,-1.3364522457
H,0,-1.5970533535,-1.0917214416,2.1938792256
H,0,-2.7943320102,1.1952368165,1.3378819831

5‡

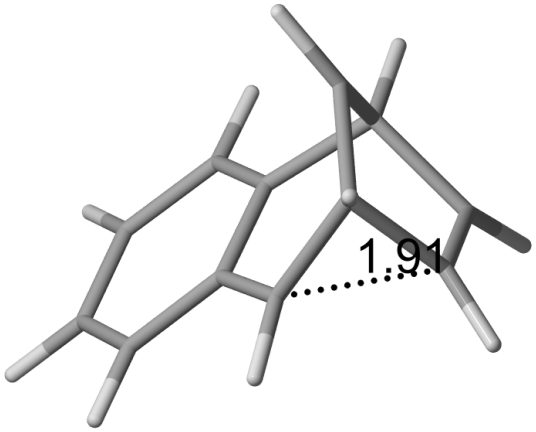

/home/hanyclose/dipimethane/paper/DPM-TS2
opt=(ts,calcfc,noeigentest)
E(UwB97XD) = -463.020231267

Zero-point correction= 0.178805 (Hartree/Particle)
Thermal correction to Energy= 0.186787
Thermal correction to Enthalpy= 0.187731
Thermal correction to Gibbs Free Energy= 0.145156
Sum of electronic and ZPE= -462.841426
Sum of electronic and thermal Energies= -462.833444
Sum of electronic and thermal Enthalpies= -462.832500
Sum of electronic and thermal Free Energies= -462.875075

	E	CV	S
	KCal/Mol	Cal/Mol-K	Cal/Mol-K
Total	117.211	35.195	89.608

C,0,2.8195374171,-0.6532764763,-0.0253333681
C,0,1.6154061103,-1.3563884076,0.0491120982
C,0,0.407809816,-0.672419777,0.0840094756
C,0,0.3894179784,0.7423095939,0.0613008942
C,0,1.6015705234,1.4343137993,-0.0423744725
C,0,2.8080558354,0.7402218711,-0.0778386449
C,0,-0.9715209929,-1.3358496199,0.0920586494
C,0,-0.9016271965,1.4083619501,0.1137001887
C,0,-2.1113986994,0.6778856799,0.6279451795
C,0,-1.7507334527,-0.6512708704,1.189830851
H,0,3.7614681448,-1.1921563322,-0.0512549096
H,0,1.6179371408,-2.4433639916,0.0689966798
H,0,1.5970336466,2.5205923281,-0.0781425624
H,0,3.7425792855,1.2885484843,-0.144992184
H,0,-0.8917724254,-2.4226032585,0.1762380007
H,0,-0.970470275,2.4757015046,-0.0719205025
C,0,-2.2179381271,0.4219590801,-0.8559742367
C,0,-1.6936853003,-0.8292426993,-1.1458946495
H,0,-1.5429091519,-1.2404341209,-2.1363472007
H,0,-2.7333464875,1.0818040471,-1.5407765678
H,0,-1.5862013281,-0.8396730941,2.2451135802
H,0,-2.8690224614,1.2782403094,1.1262367015

6

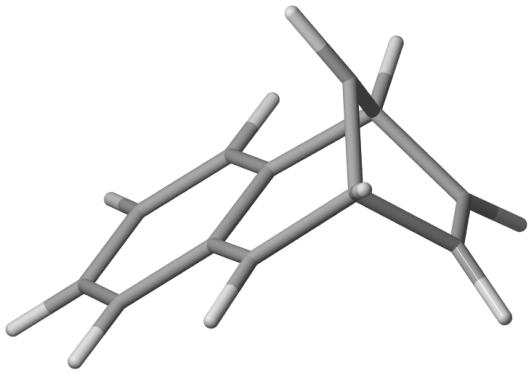

/home/hanyclose/dipimethane/paper/DPM-PD
opt
E(UwB97XD) = -463.037847860

Zero-point correction= 0.179876 (Hartree/Particle)
Thermal correction to Energy= 0.188287
Thermal correction to Enthalpy= 0.189232
Thermal correction to Gibbs Free Energy= 0.145841
Sum of electronic and ZPE= -462.857972
Sum of electronic and thermal Energies= -462.849560
Sum of electronic and thermal Enthalpies= -462.848616
Sum of electronic and thermal Free Energies= -462.892007

	E	CV	S
	KCal/Mol	Cal/Mol-K	Cal/Mol-K
Total	118.152	36.667	91.323

C,0,-2.8164379541,-0.6586040108,0.1198269053
C,0,-1.5909144835,-1.327458918,0.0456664861
C,0,-0.4030319874,-0.6252645375,-0.0860026208
C,0,-0.4244771264,0.806827248,-0.168152756
C,0,-1.6779762767,1.4602354077,-0.0747683919
C,0,-2.851901798,0.7385575629,0.0631359888
C,0,0.9658878771,-1.3075385258,-0.1300718492
C,0,0.7863927022,1.5240545151,-0.3413678454
C,0,2.0891815271,0.7458879256,-0.4193218935
C,0,1.7794135717,-0.5415952467,-1.1393020725
H,0,-3.7369519125,-1.2238560314,0.2254876778
H,0,-1.5638040889,-2.4130485189,0.0985076195
H,0,-1.70755167,2.5454764695,-0.1255366777
H,0,-3.80241861,1.2593820659,0.1245661708
H,0,0.8625836986,-2.3793349026,-0.319752465
H,0,0.7852161151,2.6103558894,-0.3491064886
C,0,2.3596149313,0.2039610903,0.9915407698
C,0,1.7155973927,-0.9539282259,1.1537885516
H,0,1.6274803513,-1.5228351181,2.0722110948
H,0,2.8956708631,0.7607746075,1.7515385017
H,0,1.6092909118,-0.598093147,-2.2102887006
H,0,2.8973259653,1.3446984007,-0.8453140057

7

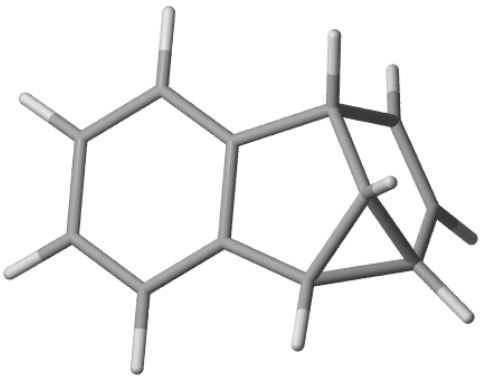

opt
E(UwB97XD) = -463.114940909

Zero-point correction= 0.183764 (Hartree/Particle)
Thermal correction to Energy= 0.191502
Thermal correction to Enthalpy= 0.192446
Thermal correction to Gibbs Free Energy= 0.151202
Sum of electronic and ZPE= -462.931177
Sum of electronic and thermal Energies= -462.923439
Sum of electronic and thermal Enthalpies= -462.922495
Sum of electronic and thermal Free Energies= -462.963738

	E	CV	S
	KCal/Mol	Cal/Mol-K	Cal/Mol-K
Total	120.169	34.082	86.804

C,0,-2.7726161279,-0.6393735755,0.4275024392
C,0,-1.5928073691,-1.3593665739,0.2199481043
C,0,-0.4570282231,-0.6784520987,-0.1946038247
C,0,-0.4812731505,0.7136130805,-0.3767312364
C,0,-1.6466192452,1.4317957912,-0.140969457
C,0,-2.7971499379,0.7441373879,0.2538588996
C,0,0.9706610016,-1.1834382647,-0.3680230035
C,0,0.8344877204,1.185012984,-0.8731842385
C,0,2.1549627599,0.9000107297,-0.086160606
C,0,1.6653404805,-0.0393238995,-1.1496918873
H,0,-3.6769088187,-1.1610455569,0.7255180529
H,0,-1.5712835021,-2.4352827501,0.370647931
H,0,-1.6695399661,2.5094824835,-0.2755294482
H,0,-3.7199059984,1.2910273935,0.4215551214
H,0,1.0541515747,-2.1780874445,-0.8107954786
H,0,0.8715553002,2.0459621444,-1.5330844176
C,0,2.1232393888,0.1531924294,1.1969601471
C,0,1.5483301918,-1.04491464,1.0385163869
H,0,1.3291930699,-1.7545692094,1.829154848
H,0,2.4867617755,0.5589373892,2.134176291
H,0,2.1851149502,-0.2111115561,-2.0855895158
H,0,2.9595241254,1.6004487557,-0.2861891078

8

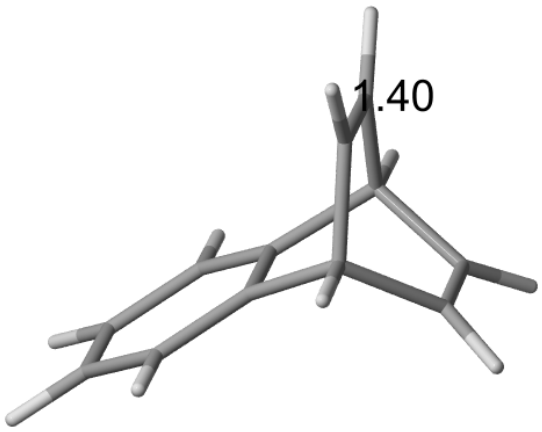

After scan r=1.3997 d=0.0471
freq=hpmodes
E(UwB97XD) = -462.989420116

Zero-point correction= 0.177365 (Hartree/Particle)
Thermal correction to Energy= 0.185169
Thermal correction to Enthalpy= 0.186113
Thermal correction to Gibbs Free Energy= 0.143677
Sum of electronic and ZPE= -462.812055
Sum of electronic and thermal Energies= -462.804251
Sum of electronic and thermal Enthalpies= -462.803307
Sum of electronic and thermal Free Energies= -462.845743

	E	CV	S
	KCal/Mol	Cal/Mol-K	Cal/Mol-K
Total	116.195	33.259	89.315

C	-2.743379	0.694543	0.000946
C	-1.532546	1.402157	0.000026
C	-0.341567	0.699843	0.000896
C	-0.341564	-0.699835	0.000875
C	-1.532543	-1.402149	-0.000010
C	-2.743376	-0.694537	0.000929
C	1.074776	1.284763	-0.001432
C	1.074779	-1.284767	-0.001408
C	1.756653	-0.699839	1.230648
C	1.756653	0.699852	1.230634
H	-3.683781	1.236968	0.001568
H	-1.532080	2.488890	-0.000949
H	-1.532078	-2.488882	-0.000994
H	-3.683778	-1.236964	0.001545
H	1.073866	2.375387	-0.016461
H	1.073855	-2.375390	-0.016413
C	1.754473	-0.665107	-1.229189
C	1.754421	0.665075	-1.229228
H	2.164143	1.289639	-2.014198
H	2.164228	-1.289683	-2.014131
H	2.167796	1.318221	2.018771
H	2.167149	-1.318193	2.019135

References

1. DIELS-ALDER ADDITION OF PERCHLOROBENZYNE: BENZOBARRELENE. Org. Synth. 1979, 59, 71. https://doi.org/10.15227/orgsyn.059.0071.

2. Zimmerman, H. E.; Givens, R. S.; Pagni, R. M. The Photochemistry of Benzobarrelene. Mechanistic and Exploratory Photochemistry. XXXV. *J. Am. Chem. Soc*. **1968**, *90*, 6096–6108. https://doi.org/10.1021/ja01024a029.

3. Frisch, M. J.; Trucks, G. W.; Schlegel, H. B.; Scuseria, G. E.; Robb, M. A.; Cheeseman, J. R.; Scalmani, G.; Barone, V.; Petersson, G. A.; Nakatsuji, H.; Li, X.; Caricato, M.; Marenich, A. V.; Bloino, J.; Janesko, B. G.; Gomperts, R.; Mennucci, B.; Hratchian, H. P.; Ortiz, J. V.; Izmaylov, A. F.; Sonnenberg, J. L.; Williams; Ding, F.; Lipparini, F.; Egidi, F.; Goings, J.; Peng, B.; Petrone, A.; Henderson, T.; Ranasinghe, D.; Zakrzewski, V. G.; Gao, J.; Rega, N.; Zheng, G.; Liang, W.; Hada, M.; Ehara, M.; Toyota, K.; Fukuda, R.; Hasegawa, J.; Ishida, M.; Nakajima, T.; Honda, Y.; Kitao, O.; Nakai, H.; Vreven, T.; Throssell, K.; Montgomery Jr., J. A.; Peralta, J. E.; Ogliaro, F.; Bearpark, M. J.; Heyd, J. J.; Brothers, E. N.; Kudin, K. N.; Staroverov, V. N.; Keith, T. A.; Kobayashi, R.; Normand, J.; Raghavachari, K.; Rendell, A. P.; Burant, J. C.; Iyengar, S. S.; Tomasi, J.; Cossi, M.; Millam, J. M.; Klene, M.; Adamo, C.; Cammi, R.; Ochterski, J. W.; Martin, R. L.; Morokuma, K.; Farkas, O.; Foresman, J. B.; Fox, D. J. Gaussian 16 Rev. C.01; Wallingford, CT, 2016.

4. Neese, F. (2018). "Software update: The ORCA program system, version 4.0". Wiley Interdiscip Rev Comput Mol Sci. 8 (1): e1327. doi:10.1002/wcms.1327

5. Zheng, J.; Bao, J. L.; Zhang, S.; Corchado, J. C.; Meana-Paneda, R.; Chuang, Y. -Y.; Coitino, E. L.; Ellingson, B. A.; Truhlar, D. G. GAUSSRATE, version 2017/P2017-G09 University of Minnesota: Minneapolis, MN, 2017.

6. Zheng, J.; Bao, J. L.; Meana-Pañeda, R.; Zhang, S.; Lynch, B. J.; Corchado, J. C.; Chuang, Y.-Y.; Fast, P. L.; Hu, W.-P.; Liu, Y.-P.; Lynch, G. C.; Nguyan, K. A.; Jackels, C. F.; Fernandez Ramos, A.; Ellingson, B. A.; Melissas, V. S.; Villà, J.; Rossi, I.; Coitiño, E. L.; Pu, J.; Albu, T. V.; Ratkiewicz, A.; Steckler, R.; Garrett, B. C.; Isaacson, A. D.; and Truhlar, D. G.; Polyrate–version 2016-2A, University of Minnesota, Minneapolis, 2016.